

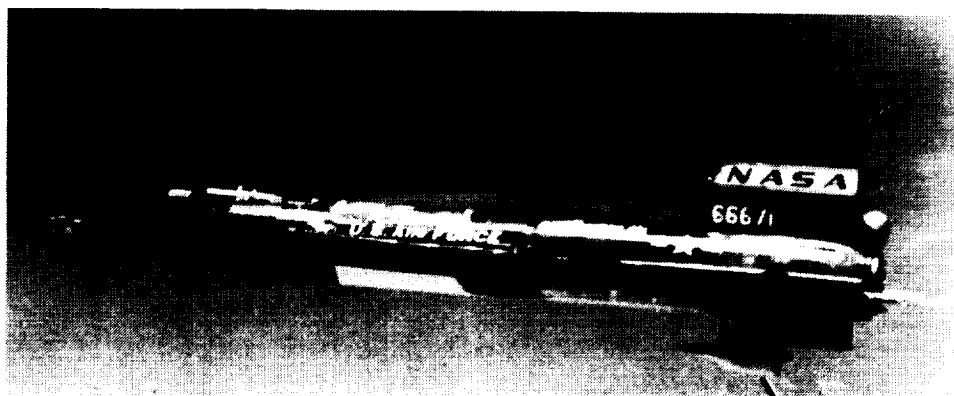
N93-12458

ACTIVE COOLING FROM THE SIXTIES TO NASP

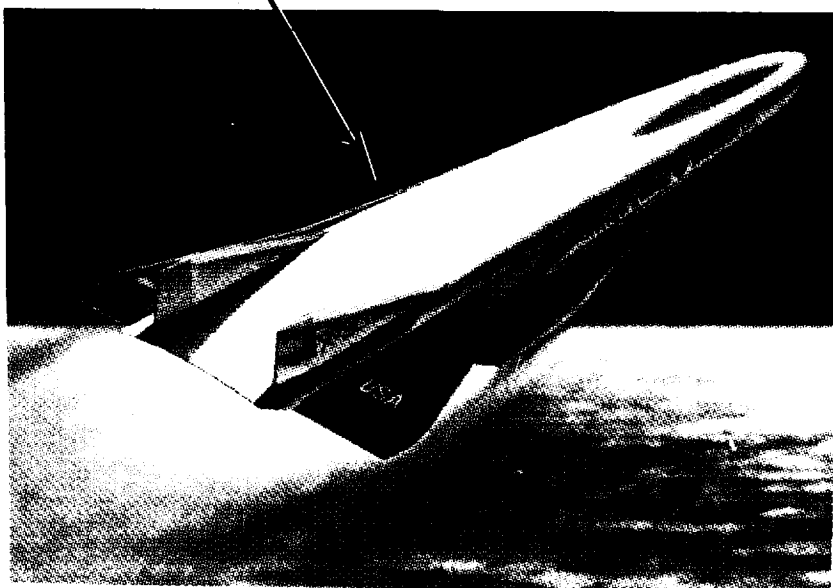
H. Neale Kelly and Max L. Blosser

INTRODUCTION

Vehicles, such as the X-15 or National Aero-Space Plane shown in figure 1, traveling at hypersonic speeds through the earth's atmosphere experience aerodynamic heating. The heating can be severe enough that a thermal protection system is required to limit the temperature of the vehicle structure. Although several categories of thermal protection systems are mentioned briefly, the majority of the present paper describes convectively cooled structures for large areas. Convective cooling is a method of limiting structural temperatures by circulating a coolant through the vehicle structure. Efforts to develop convectively cooled structures during the past 30 years — from early engine structures, which were intended to be tested on the X-15, to structural panels fabricated and tested under the National Aero-Space Plane (NASP) program — are described. Many of the lessons learned from these research efforts are presented.



X15/Hypersonic Research Engine



National Aero-space Plane

Figure 1

THERMAL PROTECTION SYSTEM CONCEPTS

Hypersonic vehicles encountering severe enough aerodynamic heating require a thermal protection system (TPS) to limit structural temperatures to acceptable levels. The type of TPS required depends largely on the magnitude and duration of the surface heating. Because the heating varies over the surface of a vehicle, several different types of TPS may be used on the same vehicle. Some of the TPS concepts which have been considered are indicated schematically in figure 2. The concepts are divided into three broad categories: passive, semi-passive and active. As defined in figure 2, passive concepts have no working fluid to remove heat — the heat is either radiated from the surface or absorbed in the structure. Semi-passive concepts have a working fluid which removes heat from the point of application, but require no external systems to provide or circulate the coolant during flight. Active concepts have an external system which provides coolant during the flight to continually remove heat from the structure or prevent heat from reaching the structure.

The simplest, lightest weight TPS concept which will accommodate the design surface heating is generally selected. The concepts, shown schematically in figure 2, are arranged in approximate order of increasing heat load capability. The passive systems are the simplest, but have the lowest heat load capability. The heat sink concept absorbs almost all the incident heat and stores it in the structure. Additional thermal mass may be added to increase the heat storage capability, but the concept is limited to short heat pulses. A hot structure design allows the structural temperature to rise until the heat being radiated from the surface is equal to the incident heating. This concept is not limited by the duration of the heat pulse, but is limited by the acceptable surface temperature for proposed materials. Currently, carbon-carbon material, which has the highest operating temperature of the materials being considered for hot structures is limited by its oxidation resistant coating to a maximum temperature of about 3000°F (this surface temperature corresponds to a radiation equilibrium heat flux of 55 Btu/ft²-sec for a surface emittance of 0.8). Insulation systems have features of both heat sink and hot structure. The surface becomes hot and radiates away most of the incident heating. Insulation prevents all but a fraction of the incident heating from reaching the underlying structure. The structure acts as a heat sink to store the heat that reaches it. Although both the magnitude and duration of the heating are limited for insulated systems, lower temperature structural materials can be used.

Two semi-passive concepts are illustrated in figure 2. Heat pipes are attractive for areas where there is a localized area of high heating with an adjacent area of low heating (below radiation equilibrium temperature for the heat pipe material). Heat is absorbed into the heat pipe at the highly heated area. The absorbed heat vaporizes a working fluid. The resulting vapor flows to a cooler region where it condenses and the heat is rejected. The condensed working fluid is returned to the highly heated region by capillary action. Ablators undergo a chemical reaction which generates gases that block much of the aerodynamic heating to the vehicle surface. However, the ablator is consumed in the process, thus requiring refurbishment and limiting the duration of its operation.

Three active cooling concepts are shown in figure 2. Both transpiration and film cooling operate on a principle similar to that of ablation — coolant ejected from the surface blocks most of the aerodynamic heating from reaching the structure. These two concepts use an external pumping system to bring the coolant from a remote reservoir and eject it from the surface. Transpiration cooling involves ejecting the coolant through a porous surface, whereas film cooling involves ejecting the coolant essentially parallel to the flow from discrete slots. The mass penalties associated with the expendable coolant usually

limit these concepts to small, highly heated regions. Convective cooling is accomplished by circulating coolant through passages in the structure to remove the absorbed heat due to aerodynamic heating. Almost all of the incident heating is transferred through the outer skin into the coolant. If the heat is transferred to the fuel before it is burned, the system is called a regenerative cooling system. Development of convectively cooled structures is the subject of the present paper and the following figures illustrate some of the fundamental issues which must be addressed to design such structures.

THERMAL PROTECTION SYSTEM CONCEPTS

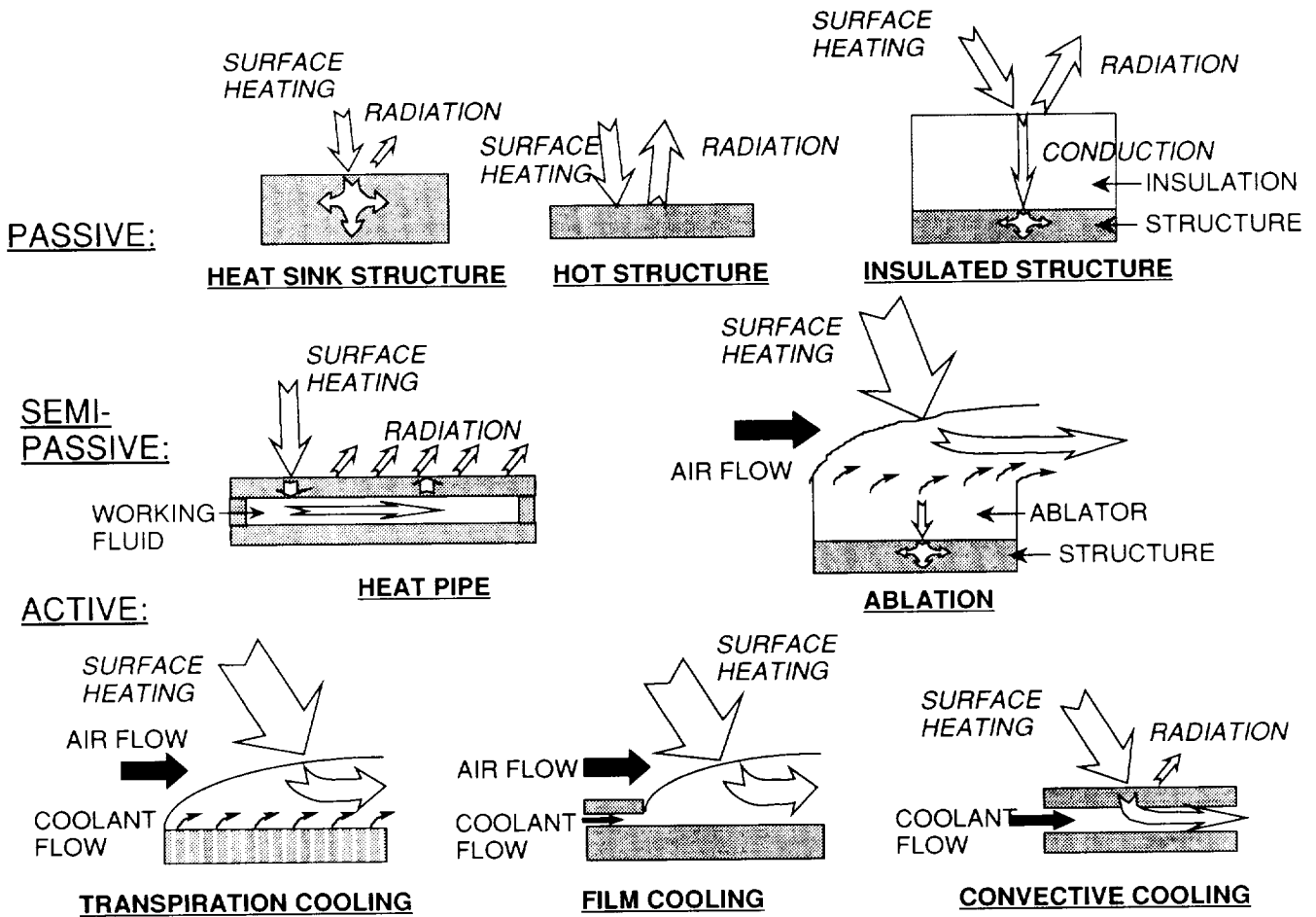


Figure 2

CONVECTIVELY COOLED STRUCTURE

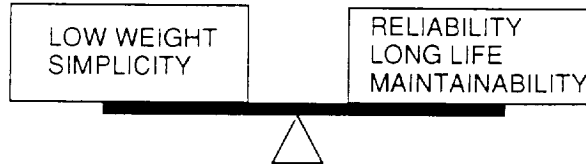
Design of convectively cooled structures requires balancing sometimes conflicting objectives. As for all aerospace structures, low weight is one of the most critical design objectives. Simplicity, reliability, long life and maintainability are also important.

Some of the fundamental design issues are illustrated in figure 3. The local thermal response of a convectively cooled structure is illustrated on the left of the figure. Most of the incident heat flux is conducted through the outer skin and transferred into the coolant, which carries it to another location on the vehicle. Because, for most actively cooled structures, the coolant keeps the surface temperature well below the radiation equilibrium temperature, the amount of heat radiated from the surface is usually considered negligible compared to the amount incident heat absorbed at the surface. The primary local thermal behavior is one dimensional and can be represented by the simple equations on figure 3. Assuming that all of the heat is conducted through the skin and is transferred into the coolant from the back surface of the skin, the temperatures can be calculated using the one-dimensional conduction and convection equations. In these equations the symbols are defined as follows: q is the heat flux; k is the thermal conductivity of the outer skin; t is the thickness of the outer skin; h is the convective heat transfer coefficient between the skin and the coolant; T_o is the temperature of the outer surface of the skin; T_i is the temperature of the inner surface of the skin; T_c is the temperature of the coolant; T_s is the temperature of the underlying structure; σ is the thermal stress in the outer skin; E is the modulus of elasticity of the skin material; and α is the coefficient of thermal expansion of the skin material. The two one-dimensional equations can be combined to produce an expression for the outer skin temperature, which is the maximum temperature of the cooled panel in this one-dimensional model. The temperature variation through the thickness of the outer skin can lead to significant thermal stresses, as illustrated on the right side of figure 3. If the outer skin were free to expand it would deform to a shape similar to that shown in the figure. However, the outer skin is usually attached to a much stiffer substructure which constrains its deformation. The outer skin can expand only as much as the substructure to which it is attached. The resulting thermal stress can be approximated by the one-dimensional equation shown in figure 3. Notice that the maximum stress depends on the difference between the outer skin temperature and the substructure temperature. If the substructure temperature is assumed to be the same as the coolant temperature, the equation for the outer skin temperature can be combined with the equation for thermal stress as shown on figure 3. From the resulting equation it can be seen that the standard practice of increasing the thickness to reduce mechanical stress would have the opposite effect for this thermal stress — the stress would increase! Therefore it is not always possible to design the skin considering only linear elastic behavior. These high local thermal stresses may lead to designs limited by more complicated material behavior such as creep and low cycle fatigue.

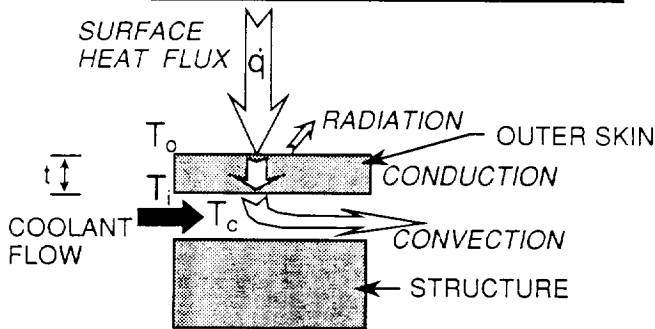
Local thermal stresses must be accommodated before a convectively cooled panel design can be successful. However, the cooled panel is only part of a cooling system and there are many other important considerations. Some of the other components of a cooling system are illustrated in the next figure.

CONVECTIVELY COOLED STRUCTURE

OBJECTIVES:



LOCAL THERMAL RESPONSE



1-D Conduction

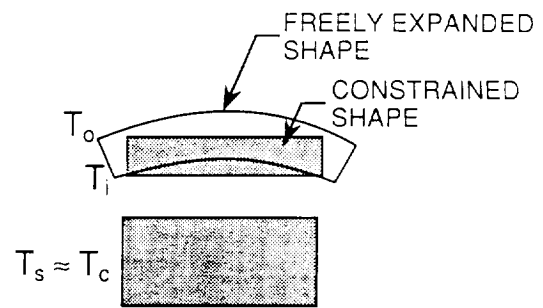
$$\dot{q} = \frac{k}{t}(T_o - T_i)$$

1-D Convection

$$\dot{q} = h(T_i - T_c)$$

$$T_o = \dot{q} \left(\frac{t}{k} + \frac{1}{h} \right) + T_c$$

LOCAL STRUCTURAL RESPONSE



1-D Thermal Stress

$$\sigma_{\max} = E \alpha (T_o - T_s)$$

$$\sigma_{\max} = E \alpha \dot{q} \left(\frac{t}{k} + \frac{1}{h} \right)$$

Figure 3

CONVECTIVE COOLING SYSTEMS

Two different convective cooling systems are shown in figure 4: direct hydrogen cooling and indirect cooling. In the direct cooling system the hydrogen fuel flows directly through the cooled panel enroute to the engine to be burned. In the indirect system a secondary coolant, which may be a more easily pumped liquid instead of hydrogen, circulates through the cooled panel and then through a heat exchanger which transfers the heat to the hydrogen fuel. For both systems the heat transferred to the fuel has a beneficial effect on the combustion process. Because the heat is used rather than simply rejected overboard, this type of cooling is sometimes called regenerative cooling. Both systems circulate the coolant through many small passages in a cooled panel. An inlet manifold is required to feed coolant into the multiple passages and an outlet manifold is needed to remove coolant from the passages. Plumbing and a pump are necessary to route the coolant to and from the cooled panel. For the indirect cooling system an additional pump, a heat exchanger, and perhaps a secondary coolant reservoir may also be required. All of these items add complexity and weight, but are essential if an actively cooled structure is required to accommodate the aerodynamic or combustion heat loads. Also, some systems are designed with redundant coolant circuits in an attempt to increase reliability. However, this redundancy results in an increase in weight and complexity.

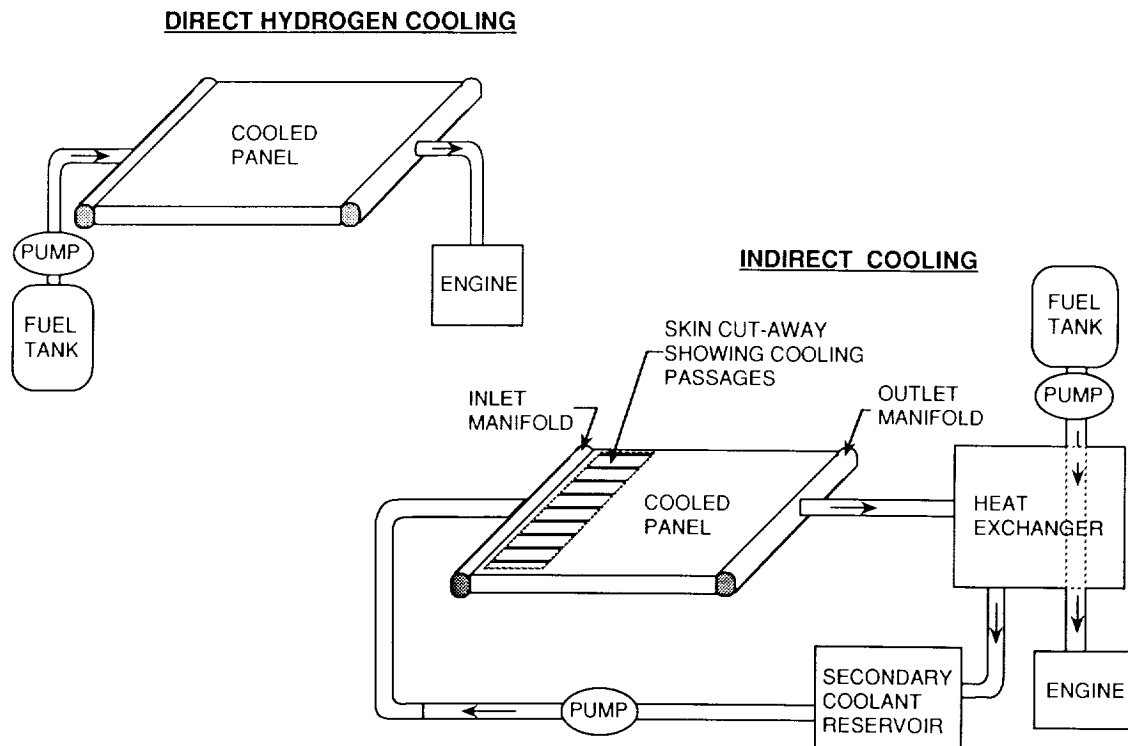


Figure 4

TIME LINE FOR DEVELOPMENT OF CONVECTIVELY COOLED STRUCTURES

A time line for the development of convectively cooled structures is shown in figure 5. During the late 1950's and 1960's there was considerable interest, both in NASA and the Air Force, in hypersonic vehicles. This interest included extensive system studies and, in some cases, the development and testing of convectively cooled structures. Unfortunately, the Air Force interest in hypersonics waned in the mid to late 1960's.

There has been continuous interest in both the Air Force and NASA in cooled structures for rockets. However, these are relatively short lived structures compared with the structure required for engines and airframes of hypersonic cruise type vehicles. Most of the cooled structures research for hypersonic cruise vehicles during the 1970's and early 1980's was at the Langley Research Center — although there was continuing interest in hypersonic cruise missiles at the Johns Hopkins Applied Physics Laboratory. Research on hypersonics reached a low ebb during the late 1970's and early 1980's. Subsequently, the advent of the National Aero-Space Plane (NASP) has led to a resurgence of interest in hypersonics.

The sections that follow provide a somewhat cursory review of the development of actively cooled structures (primarily at the Langley Research Center) and a summary of lessons learned over the past thirty years. Some of the early work was reported at the 1967 Hypersonics Conference (ref. 1). Much of the engine and airframe work, with the exception of the Hypersonic Research Engine (HRE) effort was reviewed at a 1978 symposium (ref. 2). The HRE work is reported in references 3 and 4. All of the previous work was summarized in papers by Wieting, Shore, McWithey, and Kelly at the First National Aero-Space Plane Symposium (ref. 5). The NASP actively cooled structures effort was reviewed by Kelly et al in papers presented at the Tenth National Aero-Space Plane Symposium (ref. 6) and a Society for Experimental Mechanics Testing Conference (ref. 7).

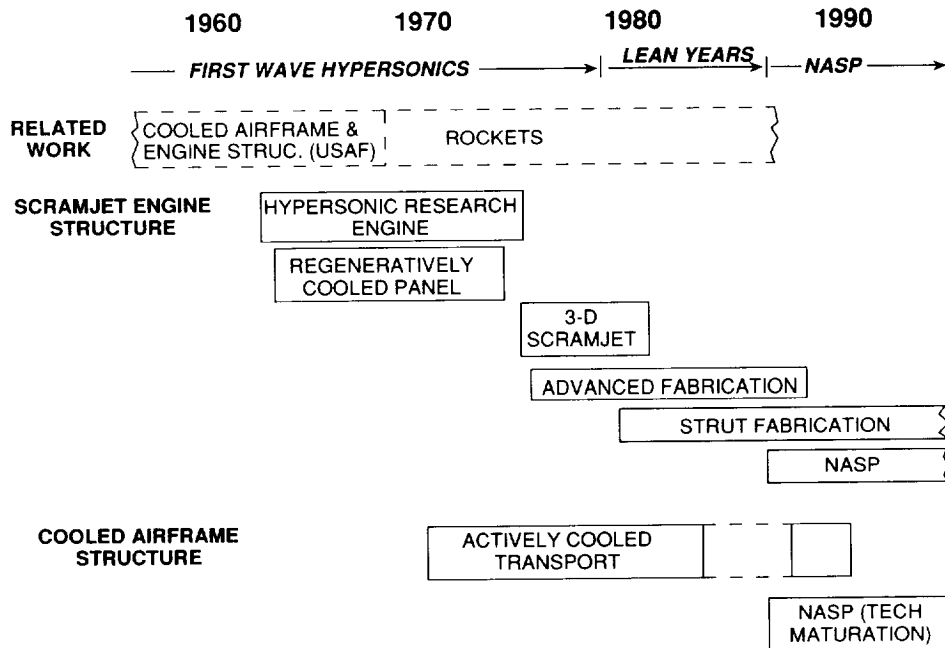
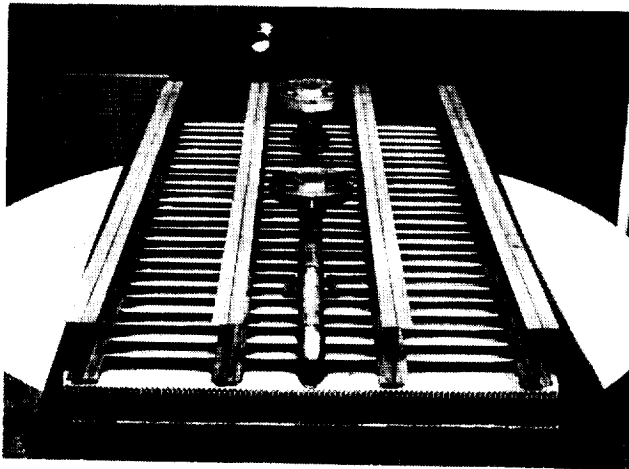


Figure 5

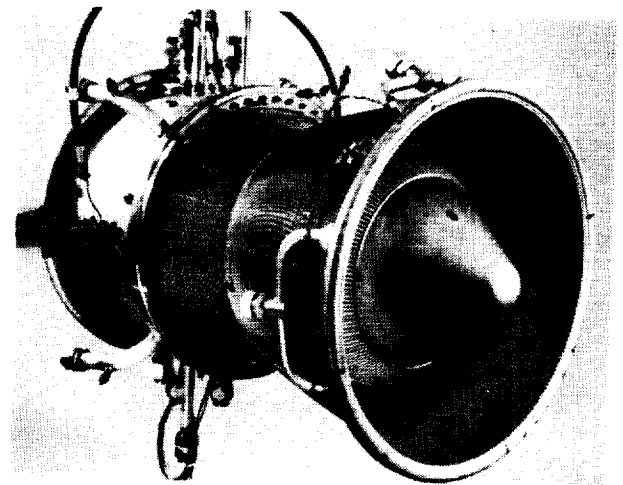
AIR FORCE ACTIVELY COOLED STRUCTURE

The level of sophistication reached by the early Air Force sponsored actively cooled structure development is illustrated by figure 6. An actively-cooled structural panel fabricated by Bell Aerosystems and a cooled engine test rig, fabricated by the Marquart Company as part of the Air Force hypersonic ramjet propulsion project are shown. The design and fabrication of a two by four foot, flat, hydrogen-cooled panel made of a superalloy, Haynes L-605, is documented in reference 8. An extensive reference list of some of the early Air Force cooling studies is also contained in reference 8. Unfortunately, because of waning interest in hypersonics, the Haynes L-605 panel, which developed leaks during proof pressure tests, was never tested.

As part of the Air Force's hypersonic ramjet propulsion program, a 20-inch-diameter by 30-inch-long regeneratively cooled combustion chamber and nozzle was fabricated and tested in a direct connect duct mode. (Air at temperatures, pressures, and flow rates representative of conditions exiting the inlet is supplied by the test facility through a duct connected to the combustor.) This test rig featured a brazed contoured Hastelloy X, D-shaped, cooling tube bundle wall with a Rene' 41 structural overwrap (ref. 9). The combustion chamber and nozzle specimen was exposed to conditions representative of Mach 4 to 6 operation and accumulated a total testing time of approximately one half hour, but was never exposed to the maximum design conditions — Mach 8 with the coolant flow rate equal to the fuel flow rate.



Hydrogen Cooled Panel of
L-605 Alloy



Hypersonic Ramjet Development Engine
2 Jul 68

Figure 6

REGENERATIVELY COOLED ENGINE STRUCTURES

Activity concerned with regeneratively cooled, air-breathing propulsion structures at NASA Langley Research Center is depicted in figure 7. In the 1960's Langley sponsored two comprehensive studies of hydrogen-cooled engine structures: one was a series of generic studies including thermal and structural design, fabrication, and experimental evaluation of regeneratively cooled panels (refs. 10-15); and the other involved the design, fabrication and testing of a complete Hypersonic Research Engine (HRE). The HRE project culminated in the testing of a boiler-plate, operating Aerothermodynamic Integration Model (AIM) in the Hypersonic Test Facility at NASA Lewis Research Center (refs. 3 and 16) and a complete flightweight, hydrogen-cooled Structural Assembly Model (SAM) in the Langley 8-Foot High Temperature Tunnel (refs. 3, 4, and 17). The AIM tests demonstrated the internal performance of the engine at Mach numbers of 5, 6, and 7 and the feasibility of ramjet to scramjet transition. The SAM tests confirmed the viability of the cooled structure; however, the coolant requirements for the HRE exceeded the heat capacity of the available hydrogen fuel and the thermal fatigue life was far shorter than desired (HRE had an anticipated fatigue life of only 135 operational cycles). Both the problems stemmed, in part, from the annular design and high compression ratio of the engine which resulted in large areas being exposed to an intense heating environment. A basic goal in the continuing research program was to develop an engine concept which required only a fraction of the total fuel heat sink for engine cooling and had a reasonable fatigue life.

Findings of the HRE project and additional propulsion studies led to the development of the Langley three-dimensional, airframe integrated scramjet which features a fixed geometry, modular concept (ref. 18). In-house and industry thermal-structural design studies described in references 19 through 22 produced viable design concepts for the integrated scramjet with cooling requirements that permit engine operation to Mach numbers of 9-10 without additional hydrogen for engine cooling. However, these studies reemphasized the need for advances in fabrication and materials technology to obtain reasonable structural life. Advanced fabrication development studies to improve thermal fatigue life (ref. 23) were successful and a fuel injection strut is currently being built for tests at NASA Langley. Ultimately tests of a hydrogen-cooled duct/strut model or one or more complete engine modules are planned for the 8-Foot High Temperature Tunnel which is being modified to accommodate operating engines.

(Figure 7 is shown on the next page.)

LANGLEY ACTIVITIES ON REGENERATIVELY COOLED AIR-BREATHING PROPULSION STRUCTURE

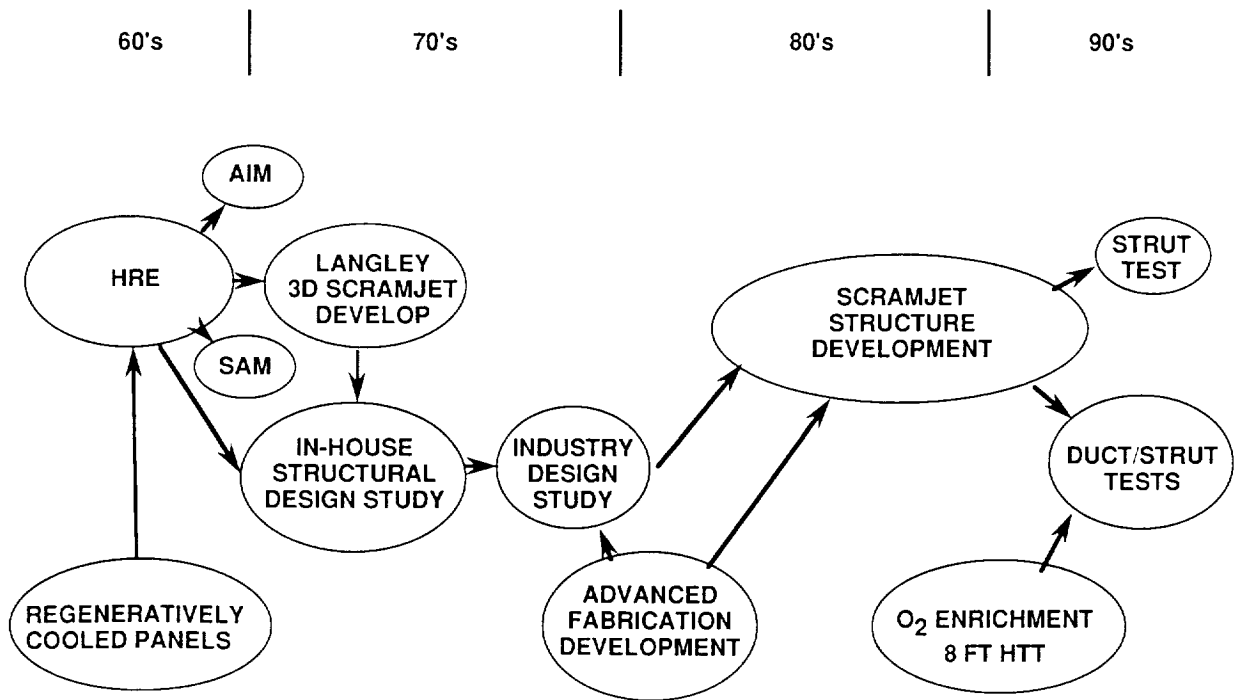


Figure 7

HYDROGEN-COOLED PROPULSION STRUCTURES

Both the regeneratively cooled panel and the HRE hydrogen-cooled structure were based on plate-fin heat exchanger technology (see figure 8) to form the cooled surfaces adjacent to the hot engine gases. These surfaces were fabricated by brazing pre-formed plain or offset fin material between cover sheets to form coolant passages. Design procedures in references 10 and 11 generally resulted in heat exchangers with very small coolant passages, as indicated by the photograph. An appreciation of the passage size can be gained by comparing the passages with the paper clip shown in figure 8. Because of the close spacing of the fins, foil-gage materials can be used to contain coolant pressures in excess of 1000 psi with surface temperatures of 2000°R. The offset fins promote heat transfer to the coolant and reduce the temperature difference between the heat exchanger surfaces, thereby reducing through-the-thickness thermal stresses.

TYPICAL HYDROGEN HEAT EXCHANGER

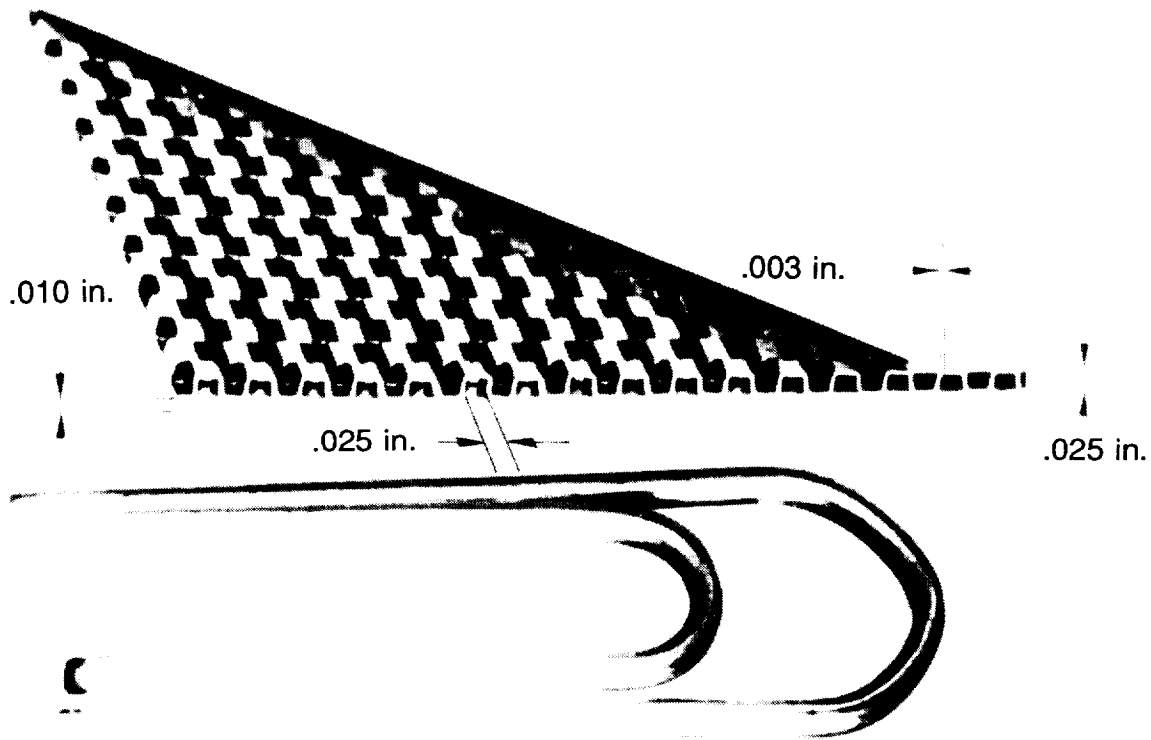


Figure 8

COOLED STRUCTURE CONCEPTS

Thermal and structural design studies presented in references 10 and 11 for heat fluxes from 10 to 500 Btu/ft²-sec and external pressure loadings from 7 to 250 psi (representative of engine structures) resulted in the three preferred concepts shown in figure 9. The terms "integral", "bonded", and "non-integral" were used in the reference studies and in figure 9 to distinguish the three concepts. For the "integral" concept, channels formed by the structure are used as coolant passages. For the "bonded" concept, a hot surface heat exchanger is metallurgically attached (brazed in the reference studies) directly to the primary structural panel. For the "non-integral" configuration, a primary heat exchanger, which absorbs the majority of the incident heat, is attached to the primary structure with mechanical slip joints or attachments that flex to accommodate differences in thermal growth. A secondary heat exchanger protects the primary structure from low-level heat leaks. The "non-integral" configuration tends to minimize thermal stress, reduces interactions between thermal and mechanical loads, and permits the use of low temperature (i.e., lightweight) materials for the primary structure. The reference studies indicate that the "integral" configuration was the preferred concept at low heat fluxes and low pressures. However, the structural passages are relatively inefficient heat exchangers and for moderate to high heat fluxes and moderate pressures, the "bonded" concept is superior. At high pressures and all heat flux levels the benefits of the "non-integral" concept outweigh the complexities and it becomes the preferred choice. (Note that in some subsequent sections of the present paper, the term "integral" is applied interchangeably to both "integral" and "bonded" concepts since both must sustain the combined mechanically and thermal induced loads.)

The studies indicate that thermal stresses are a primary concern in the design of regeneratively cooled panels. In-plane thermal stresses were minimized by careful manifold design to prevent uneven distributions of flow through the panels and thus the large thermal stresses associated with nonlinear in-plane temperature gradients are avoided. Unavoidable thermal stresses, resulting from temperature variations through the thickness of the panel, were found to be minimized through the use of small coolant passages and high flow velocities which increase heat transfer and reduce temperature gradients. However, the small coolant passages and high flow velocities also result in high coolant pressure losses through the panels. For the range of coolant flow rates and pressure losses considered, the resulting through-the-thickness temperature differences made thermal fatigue a problem. Pressure containment was found to be a minor problem, and, in general, minimum-gage materials were adequate for the internal pressures considered (300 to 1000 psi).

Material selection was found to be very important in the design of regeneratively cooled panels. For the heat exchanger portion of the concepts, elevated-temperature ductility of the material was found to be a determining factor for thermal fatigue life. Uncoated nickel-base superalloys appeared to be the best candidates for hydrogen-cooled panels. Waspalloy was chosen for the integral design. Hastelloy X and Inconel 625 were best choices for the heat exchanger portion of the other two concepts. (Although limited data indicated that Inconel 625 provided slightly improved performance, Hastelloy X, which is well characterized, was used in the design studies.) A subsequent advanced fabrication study (ref. 23) found Inconel 617 and Nickel 201 to offer significant improvements in thermal fatigue life. Inconel 718 was limited for use as the primary structure only.

COOLED STRUCTURE CONCEPTS

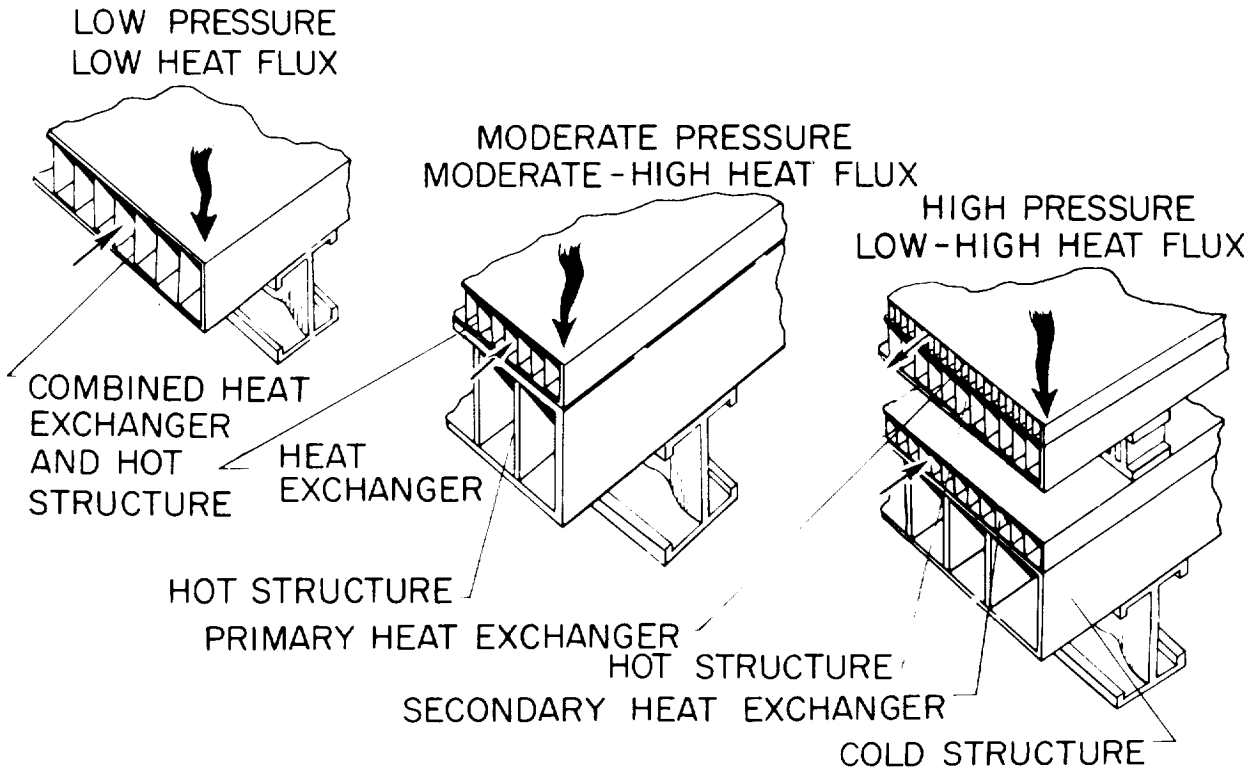


Figure 9

HYDROGEN-COOLED STRUCTURE WEIGHTS

Unit weights from the design studies of references 10 and 11 are shown for the three concepts (see figure 10) as a function of applied heat flux and external pressure loading. The weights are based on a 2- by 2-foot panel and a hydrogen outlet temperature of 1600°R. The weights include the heat exchanger, structural panels and beams, and allowances for manifolds, plumbing, and seals. Since distribution system weights and pumping penalties for the hydrogen coolant would be similar for the three concepts, these weights were ignored in the selection process. Unit weights were found to be a strong function of external pressure and a weak function of heat flux level. Shaded areas on figure 10 represent the minimum weight concept for specified pressures and heat flux. At low pressures the integral concept has the lowest weight; for higher pressures, heat transfer considerations limit the cooling fin height or depth of the panel so that the concept becomes heavier to accommodate the bending loads associated with higher pressures. At moderate pressures the bonded concept avoids the fin height problem but at the higher heat fluxes, the weight of the hot primary structure becomes excessive. For combined high heat flux and high pressure, the weight penalty for hot primary structure is greater than the weight for the additional components of the non-integral design so that the non-integral concept becomes the least-weight design.

In general, concept selection involves trades among panel weight, coolant flow rate, panel life and other factors unique to a specific mission. References 10 and 11 give detailed design information to assist in the concept selection process.

Following the thermal structural design studies, extensive fabrication and structural evaluation studies (refs. 12 and 13) were conducted for the integral and bonded heat-exchanger/hot-primary-structure concepts. Inconel 625, Hastelloy X, and Waspalloy parent metals and the Palniro family of gold-palladium-nickel braze alloys were used as materials in the studies. Tests included sheet alloy tensile tests, metallographic joint evaluations and burst, creep rupture, and cyclic flexural tests at operational temperatures. Additional information on the test and test results are given in the next figure.

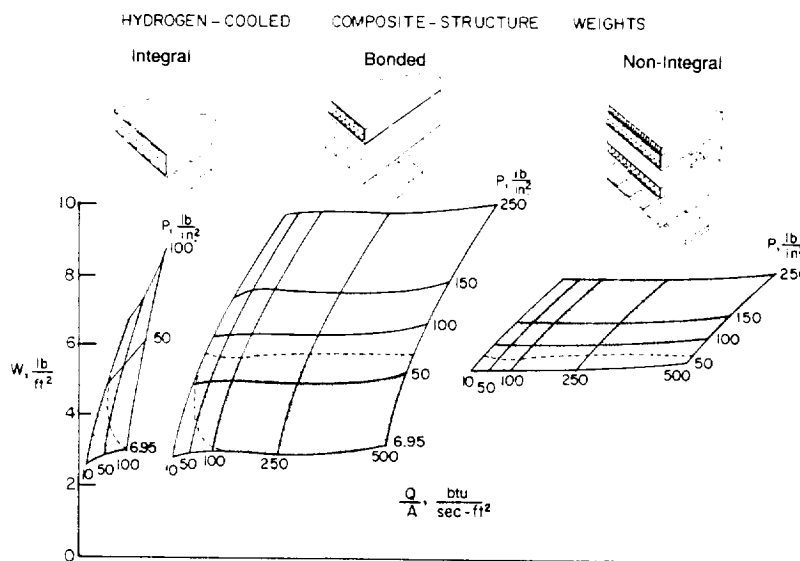


Figure 10

STRENGTH AND FATIGUE TEST RESULTS

Small 2- by 3-inch specimens were used to determine short-term burst and creep rupture properties for the plate-fin sandwich heat exchanger structures. For both types of tests the specimens were maintained at design operating temperatures in an electric furnace and pressurized with an inert gas. For the short-term burst tests, pressure was increased continuously at 20 psi/sec until failure occurred. For the rupture test, pressure was maintained at fixed levels and the specimens were allowed to creep until failure occurred. For the low-cycle fatigue test, 2- by 6-inch specimens were maintained at a test temperature of 1600°F by an electric furnace which enclosed the test apparatus as shown in figure 11. Strains were imposed mechanically by the oscillating ram and circular mandrels. Implicit in this testing method is the assumption that failure life depends on the maximum cycle temperature and cyclic strain level independent of whether the strain is mechanically or thermally induced.

Results from the tests are shown as ratios of mechanical properties of the plate-fin assemblies to the parent metal properties. The tests showed that about 85 percent of the parent metal strength was achieved in the burst tests but only 50 percent of the creep rupture strength (a 50 percent reduction in strength corresponds to a 98 percent reduction in life) and only 7 percent of the fatigue life of the parent metal could be achieved by the fabricated specimens. Many factors were found to influence the strength and fatigue life of the fabricated specimens: time at braze temperature, fin geometry, braze fillet shape, fin shape, face plate thickness, and material ductility. Creep rupture performance could be improved by increasing material gages; however, improvements in fatigue life (obtained in the integrated-scamjet development program and discussed subsequently) resulted from a redesign of the heat exchanger and the use of new fabrication techniques and better materials.

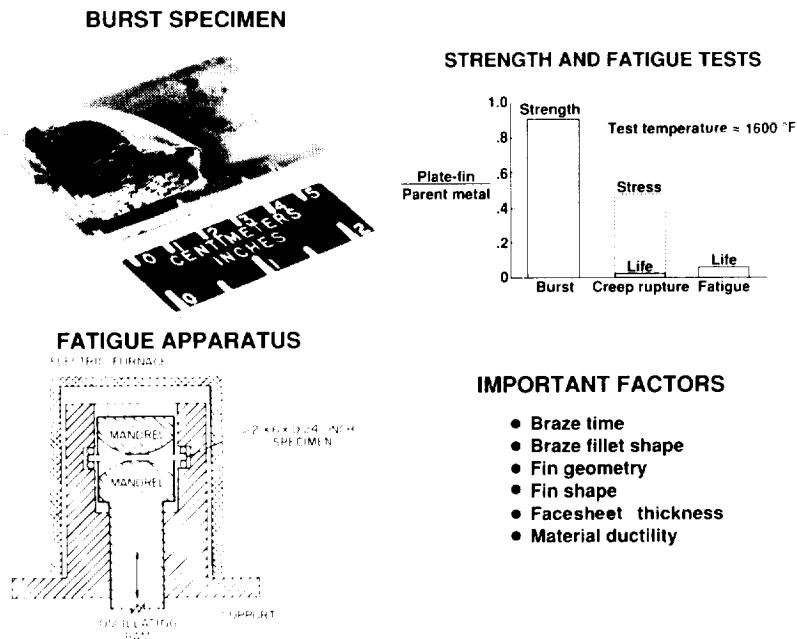


Figure 11

14- BY 20-INCH COOLED PANEL

As a culmination of the hydrogen-cooled panel studies, structural and thermal performance tests (ref. 15) were conducted on the 14- by 20-inch brazed plate-fin panel shown in figure 12. The panel consisted of an Inconel 625 heat exchanger brazed to an Inconel 718 structural panel which was supported by Inconel 718 I-beams (not shown). Clips spanning the backside of the structural panel were used to attach the panel to the I-beam supports. Inlet and outlet manifolds for distribution of the hydrogen coolant were integral parts of the structural panel. The panel was designed to sustain a 100 psi uniform surface pressure and a heat flux of 100 Btu/ft²-sec. The panel was tested in an inert gas atmosphere and a graphite heater was used to radiantly heat the cooled surface. Test conditions resulted in a maximum heat flux of 103 Btu/ft²-sec and a maximum temperature of 1470°F were imposed during the tests. A maximum uniform surface pressure of 115 psi was also applied at a temperature of 520°F. Panel heat transfer performance was generally lower than expected, apparently because of flow and heater non-uniformities. The average overall heat transfer coefficient was 63 percent of the value predicted for uniform hydrogen flow and uniform heating of the panel.

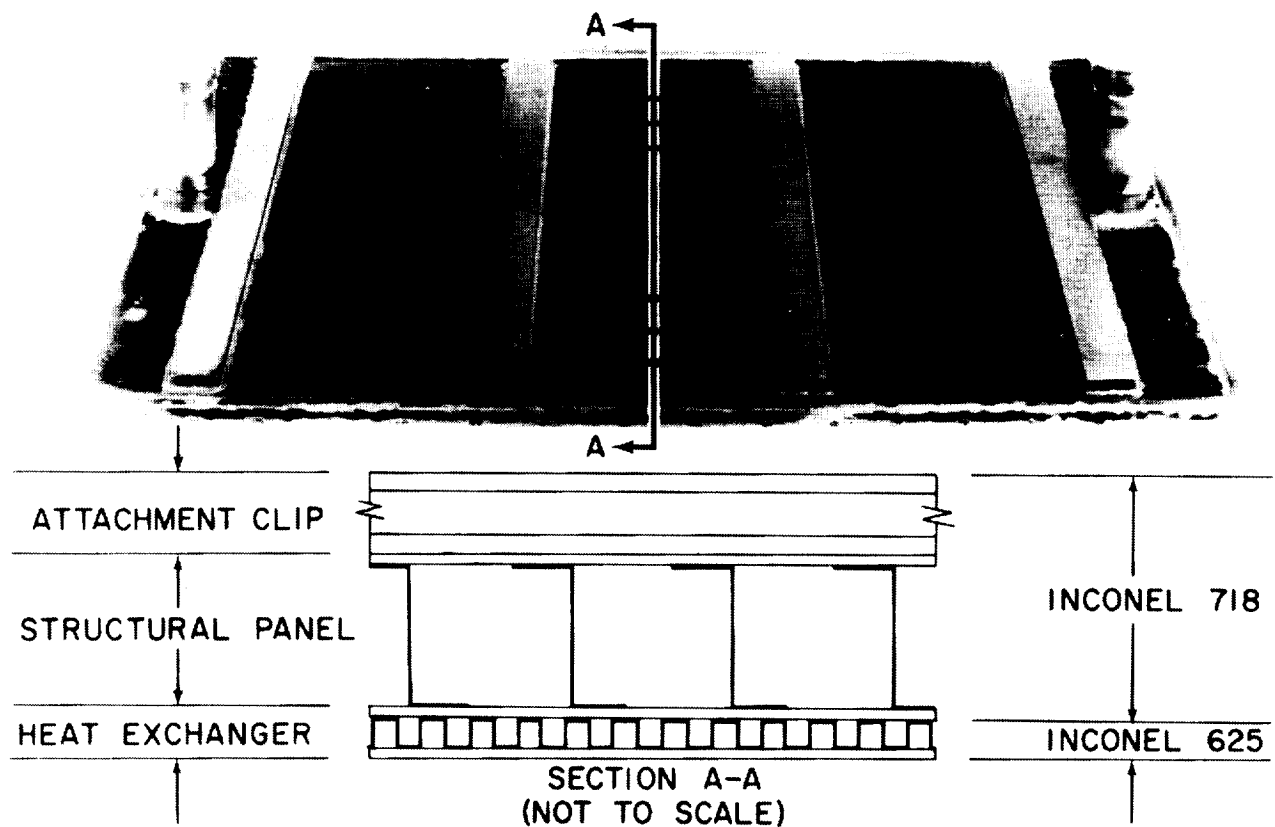


Figure 12

HYPERSONIC RESEARCH ENGINE

The Hypersonic Research Engine (HRE) was originally intended to be flight tested on the X-15 vehicle (ref. 3). The engine was designed to operate at Mach numbers from 3 to 8 at dynamic pressures up to 2000 psf. At Mach numbers above 6, it was to operate in the supersonic combustion mode. Below Mach 6 the combustion mode was not specified. HRE was to have a minimum life of 10 hours and 100 operational cycles, and to have a maximum weight of 800 pounds for compatibility with the X-15.

Subsequently, because of the demise of the X-15 project the HRE project was restructured and culminated in the testing of the boiler-plate Aerothermodynamic Integration Model (AIM) in the Hypersonic Test Facility at the Plum Brook Station of the NASA Lewis Research Center, and the flightweight, hydrogen-cooled Structural Assembly Model (SAM) in the NASA Langley Research Center 8-Foot High Temperature Tunnel. The former testing is documented in reference 16 and the latter in references 4 and 17.

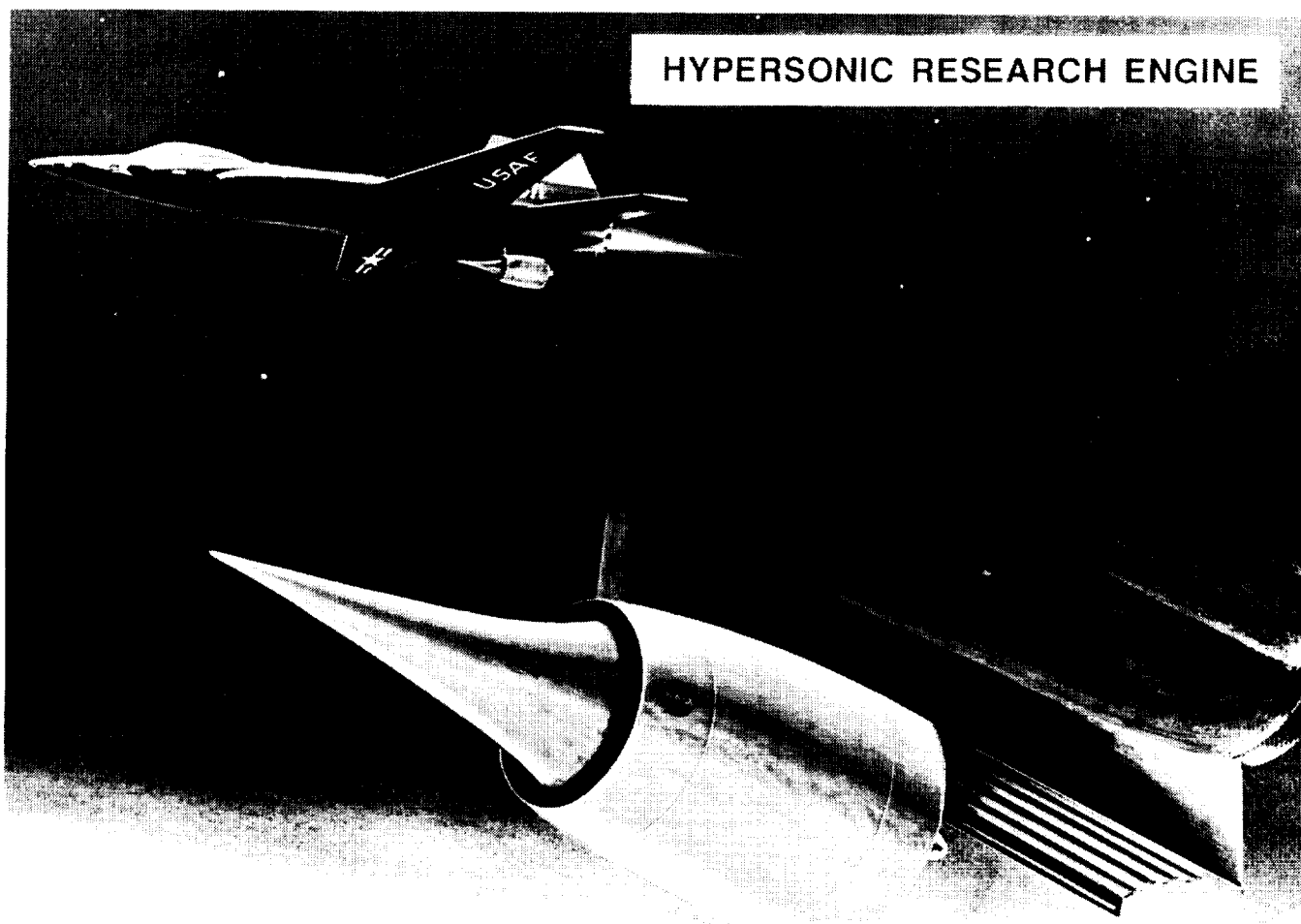


Figure 13

HRE INNER SHELL ASSEMBLY

Technology from the regeneratively cooled panel studies was incorporated in the design and fabrication of a full-scale Structural Assembly Model of the HRE engine for tests in a hypersonic flow stream. Approximately \$8 million was expended in development of hydrogen-cooled structures for the engine. Details of this development may be found in reference 24. The structure was designed for Mach 8 flight conditions and consisted of plate-fin sandwich shells with simple and compound curvatures. Use of the plate-fin sandwich construction and off-set fins resulted in a cooled structure that tolerated some blockage of flow area, permitted installation of inserts for various purposes, facilitated incorporation of manifolds into the structure, and resulted in smooth aerodynamic surfaces. The structural shells were fabricated as shown in figure 14, by laying up and brazing an assembly consisting of a precision formed Hastelloy X inner skin a layer of brazing foil, a layer of preformed Hastelloy X offset fin material, a second layer of brazing foil, and a precision formed outer skin of Hastelloy X. The final, precise shape of the inner and outer shells was obtained using successive applications of the "Electroshape" forming technique to form the outer skin, a spacer of appropriate thickness to simulate the fins and brazing material, and the inner skin in a single precision female mold. Precision forming was essential to obtain the close fit-up required for brazing. Manifolds, etc. were added during subsequent brazing operations. The Palniro family of gold-palladium-nickel brazing alloys were used because they were compatible with Hastelloy X, available in foil form and suitable for multiple brazing operations (the brazing temperature could be varied by changing the exact composition of the alloy). Five major components were mechanically joined and manifolded together to form the complete hydrogen-cooled Structural Assembly Model.

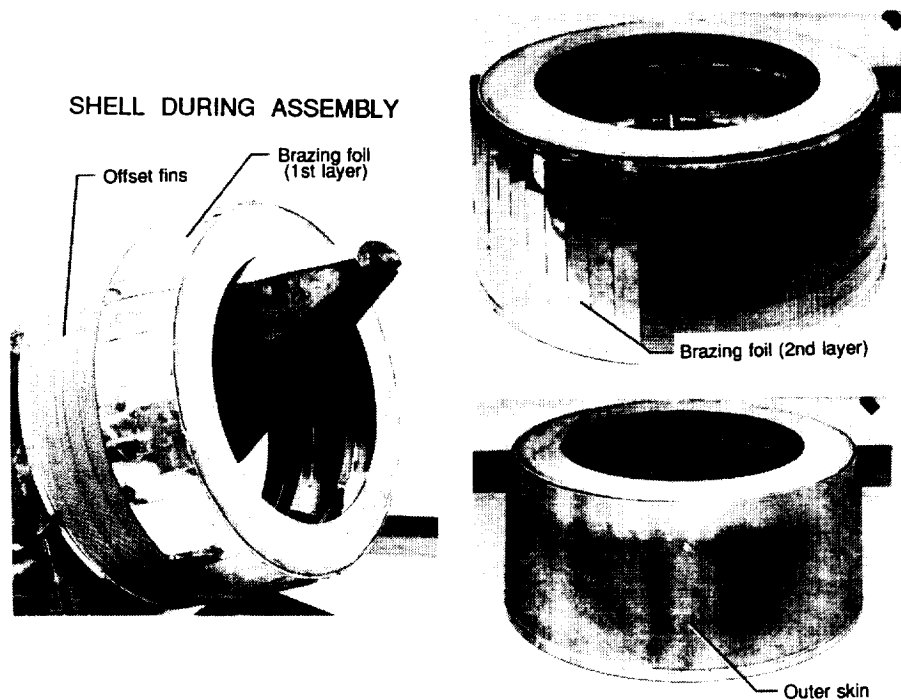


Figure 14

STRUCTURAL ASSEMBLY MODEL

Figure 15 shows the structural assembly model in the test position in the 8-Foot High Temperature Tunnel. To the right of the photograph is the 8-ft-diameter nozzle exit from which the facility derives its name. Flow in the open test section is from right to left.

The Structural Assembly Model (SAM) model was tested in the nominal Mach 7 stream of the Langley 8-Foot High Temperature Tunnel (under non-combustion conditions) for a total of 55 times to accumulate 30 minutes of exposure time which met or exceeded temperatures and temperature differences for the Mach 8 design conditions (ref. 17). Hydrogen coolant flow rates were adjusted and the transient effects of injecting a cold model into the hot test stream were used to improve the simulation of the conditions that would exist in an operating engine. Because there was no combustion in the engine during the tests, the temperature gradients resulting from steady-state wind tunnel conditions were less severe than the predicted operational gradients. However, the transient gradients resulting from introducing the unheated model into the hot airstream in the tunnel approximated the predicted steady-state operating thermal gradients. In addition, reduced coolant flow rates were used to compensate for the reduced heat fluxes in the non-operating SAM model so that the temperatures would reach the levels expected in an operating engine. Serviceability of the flight-weight plate-fin cooled structure was clearly demonstrated although the model was not tested to the full 100-cycle design life. The coolant system maintained acceptable temperature levels and tolerated large heating nonuniformities and inadvertent foreign object damage. Some minor hydrogen leakage was observed, but it was apparently inconsequential.

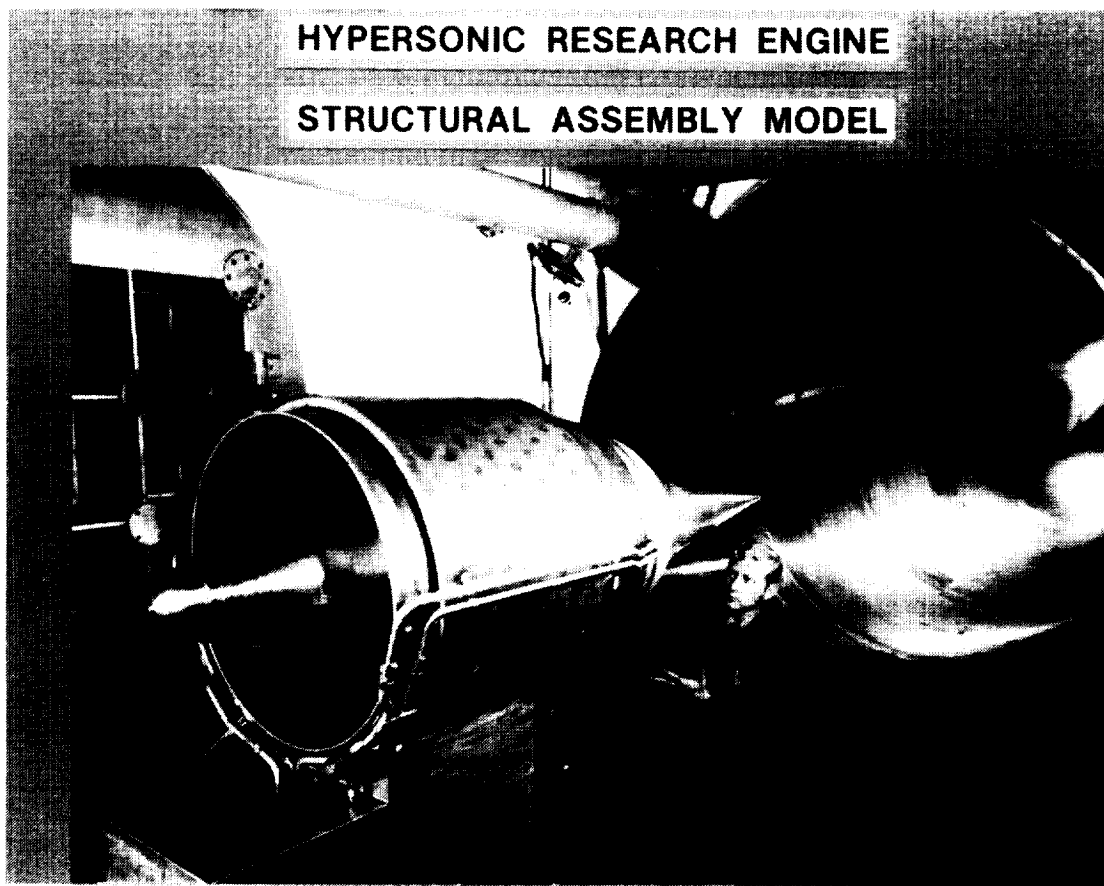


Figure 15

AIRFRAME INTEGRATED SCRAMJET

As indicated previously, the Langley Airframe Integrated Scramjet (see figure 16) was developed to overcome some of the shortcomings identified during the HRE studies: namely the limited fatigue life and the excessive coolant requirements. The modular engine uses the undersurface of the aircraft forebody to compress the flow entering the inlet and the undersurface of the afterbody to serve as an extension of the nozzle. The engine features swept compression surfaces, a cut-away cowl to permit operation over a wide range of Mach numbers, and three fuel injection struts with multiple fuel injection planes to promote and control fuel mixing and combustion. Structural advantages for this concept include, fixed geometry, minimal wetted surface area, and reduced heating rates. More detailed discussions of the conceptual design and performance may be found in reference 18.

The engine was designed to operate over a Mach number range from 4 to 10 at dynamic pressures ranging from 500 to 1500 psf. The highest heat load was encountered at Mach 10 with a dynamic pressure of 1500 psf; the most critical case for coolant/fuel matching occurred at Mach 10 with a dynamic pressure of 500 psf; and the most critical case for structural loading occurred at about Mach 5 during an engine unstart at the higher dynamic pressure (1500 psf). Design life for the LaRC scramjet was a minimum of 100 hours and 1000 thermal cycles — an order of magnitude greater than the HRE.

The salient structural design features of the Langley three-dimensional scramjet described in the figures and text to follow were derived from the Langley in-house and industry design studies. Additional details of the analysis methods, and the fuel injection strut design and fabrication are described in papers by Wieting and McWithey in reference 5. More complete descriptions of the design studies are given in references 19 through 22.

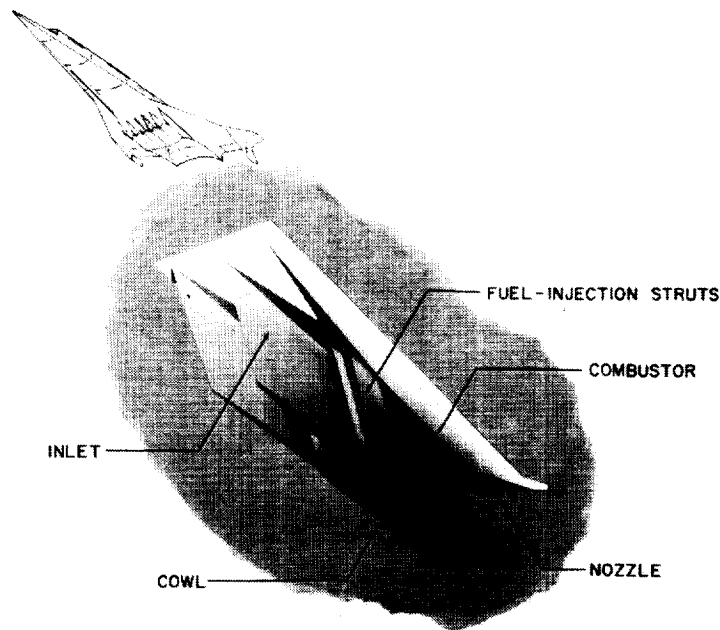


Figure 16

COOLED SCRAMJET STRUCTURE

The hydrogen-cooled scramjet structure concept which evolved from the design studies consists of a full depth brazed superalloy honeycomb structure with a brazed cooling jacket adjacent to the hot gases (see figure 17). The cooling jacket differed from that of the HRE in that fins which formed the coolant passages were photo-etched into the skin. This concept was selected primarily to increase the fatigue life (as will be discussed subsequently under advanced fabrication development); however, it also offers considerable design flexibility to meet localized requirements such as plain fins for relatively low heat flux (acreaage) areas of the engine, and offset or pin fins for high heat flux areas such as the strut. The strut and cowl featured impingement cooling of the especially high heat flux stagnation regions. The structural channels of the strut are also used to form integral manifolds for coolant and fuel distribution. Additional innovative design features of the strut are described in the paper by McWithey in reference 5.

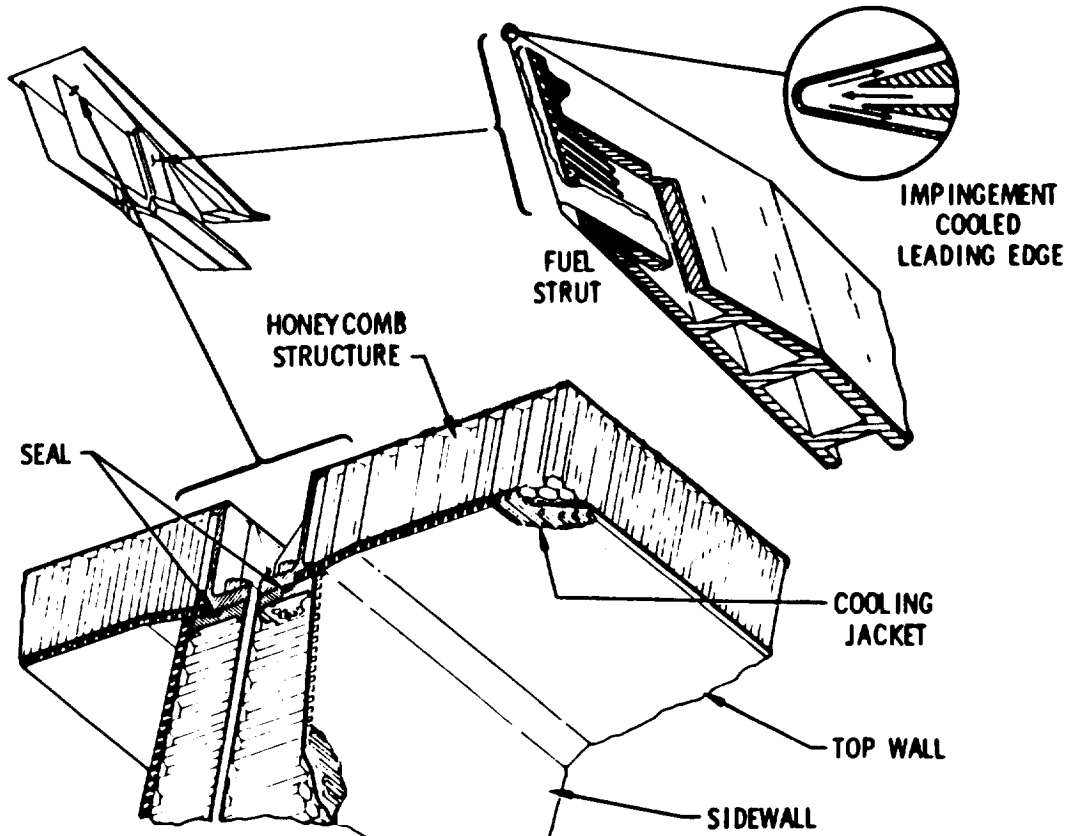


Figure 17

STUDIES OF LaRC SCRAMJET MODULE

In summary, the LaRC scramjet thermal/structural design studies which are described in detail in references 19 through 22 have shown that the basic design requirements for the scramjet can be met (see figure 18). The resulting configuration should have adequate cooling (with a coolant-to-fuel ratio ≤ 1) up to a Mach number of approximately 9-10, an expected life of at least 100 times that of the HRE, with a mass/unit-capture-area of approximately 2/3 that of HRE. (Note that the HRE was designed to a fixed weight limit and the structure was not fully optimized. However, for an annular engine the presence of the large inner body tends to negate the inherent advantages of a circular cross section for pressure containment.) The fuel injector strut, which is discussed in more detail in the paper by McWithey in reference 5, presented by far the most difficult design problem. Results of the advanced fabrication development studies, presented in the next figure, indicate that the selected cooling jacket design should meet and exceed the design life.

Thermal/Structures Studies Reveal

- 100 times life of HRE
- 2/3 mass/unit capture area of HRE
- 1/3 coolant/fuel requirement of HRE (coolant required/fuel ≤ 1.0)
- Fuel injector strut most difficult design problem

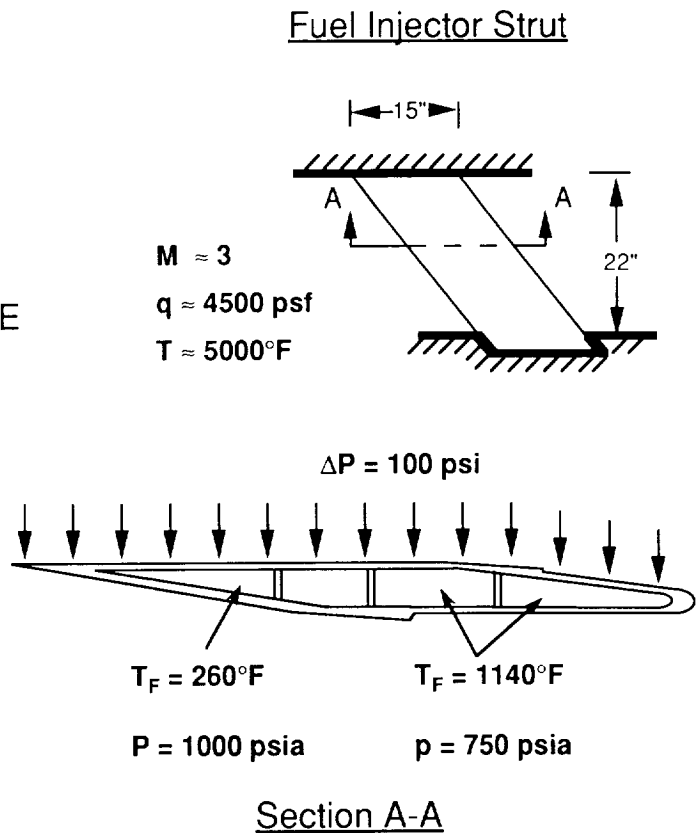


Figure 18

ADVANCED FABRICATION TECHNIQUES

Earlier studies of both the HRE and regeneratively cooled panels, indicated that, although hydrogen-cooled structures were viable, their anticipated fatigue life was extremely limited. Therefore, the advanced fabrication technique studies were undertaken with the goal of extending the usable life of cooled engine structure from the 100 cycle design life for the HRE to 1000 hours and 10,000 cycles of hot operation (cross-hatched region of figure 19) which represents an improvement of two orders of magnitude over the HRE. Predictions of the fatigue life as a function of the temperature difference between the hot aerodynamic skin and the back surface are shown in figure 19. Life goals appear attainable through a number of factors such as engine design, fabrication methods and material selection. Improvements attributable to these factors are graphically illustrated in figure 19. The bottom curve indicates anticipated life of the Hastelloy X coolant jacket of the HRE. The solid symbol at the right denotes the HRE design point and the open symbols indicate experimental data. A fundamental change in engine design to decrease the heat flux intensity and thus the temperature difference, as indicated by the horizontal arrow, is the first factor to increase the life of the airframe-integrated scramjet. An additional increase, as indicated by the vertical arrow, is obtained through an advanced fabrication technique. In this technique, the fin coolant passages are photo-chemically etched into the aerodynamic skin which eliminates the strain concentration caused by local thickening of the skin by the fin and eliminates the hot skin-to-fin braze joint configuration. However, the braze joint to the cooler primary structure is retained. The photo-chemical etching process can be used for a wide variety of plate-fin configurations. Two candidate configurations fabricated by this process are shown in figure 19. Finally, another increment in life is attained through the selection of a material with high thermal conductivity which decreases the temperature difference, and with high ductility which increases the fatigue life directly. Nickel 201 and Inconel 617 specimens were fabricated and tested and the results for Nickel 201 as indicated by the upper curve met the goal of 10,000 cycles for a design heat flux of 500 Btu/ft²-sec. Details of advanced fabrication studies, which included burst and creep-rupture evaluations in addition to fatigue evaluations, are presented in reference 23.

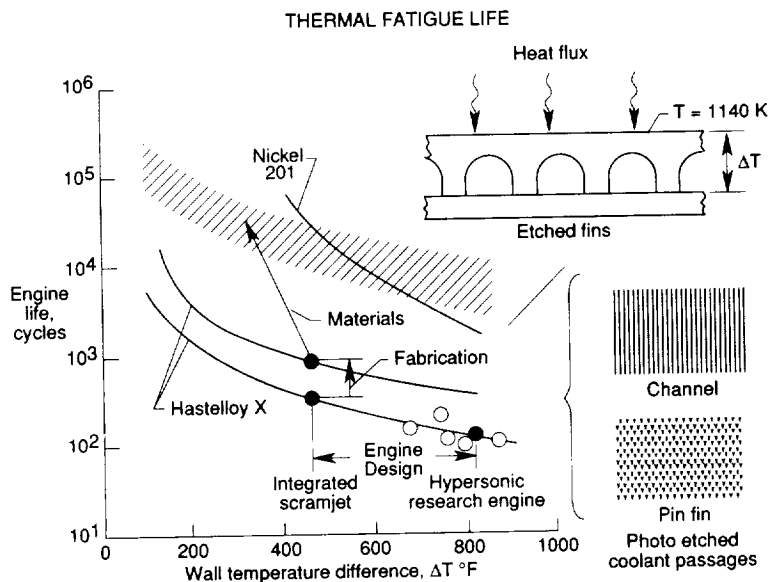


Figure 19

SCRAMJET ENGINE FUEL INJECTION STRUT

Efforts have been underway for several years to fabricate a fuel injection strut for the Langley Airframe Integrated Scramjet. The strut which is swept back 48 degrees has a 11.8-inch streamwise chord and is 28.8-inches long. The strut consists of an Inconel 718 structural body enclosed by Nickel 201 pin-fin cooling jackets.

The complexity of the strut is indicated by the cutaway mock-up on the left of figure 20. Structural cavities created by webs in the strut body form manifolds that direct hydrogen to and from the cooling jackets and manifolds that supply parallel and perpendicular fuel injectors.

Actual fabricated hardware parts are shown on the right of figure 20. The strut fabrication involves three brazing operations: (1) assembly of the strut body, (2) assembly of etched and cover sheets of the cooling jacket, and (3) final assembly of the formed cooling jackets and body. The forward jacket is shown in the formed condition and the aft jacket is shown prior to brazing to show the etched cooling passages. After forming, the cooling jackets will be hot sized to enhance fit-up between the jackets and the strut body prior to final braze.

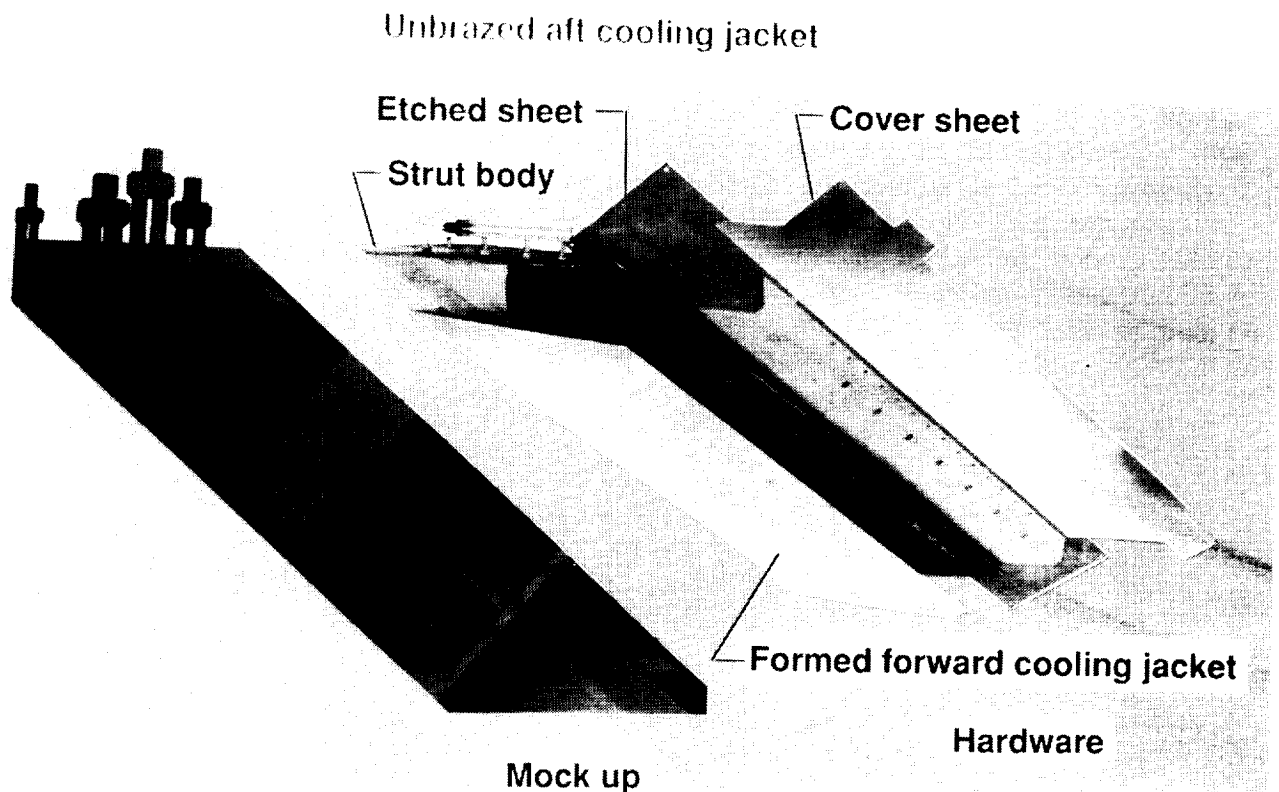


Figure 20

ACTIVELY COOLED AIRFRAME STRUCTURES

Extensive efforts have also been expended on development of secondary cooling circuit structural concepts for airframe structures (see figure 21). Systems studies indicated initial feasibility of the convective cooling approach and defined initial concepts. A series of design and fabrication studies were then conducted to further develop specific concepts. These studies included thermal-structural design, small specimen fatigue tests, fabrication development, and static and wind tunnel thermal-structural verification tests.

Although early studies for actively cooled airframe structures recognized problems in matching the instantaneous aerodynamic heat load with the heat sink capacity of the hydrogen fuel flowing to the engines and proposed partial heat shielding to reduce the absorbed heat load, both system studies (refs. 25-30) and hardware studies (refs. 31 and 32) concentrated on bare cooled structures with high-level cooling. Later studies (refs. 33-35) yielded a better understanding of the significance of heat sink matching and the mass penalties associated with high-level cooling. Selected general results from the actively cooled airframe structures studies are discussed next.

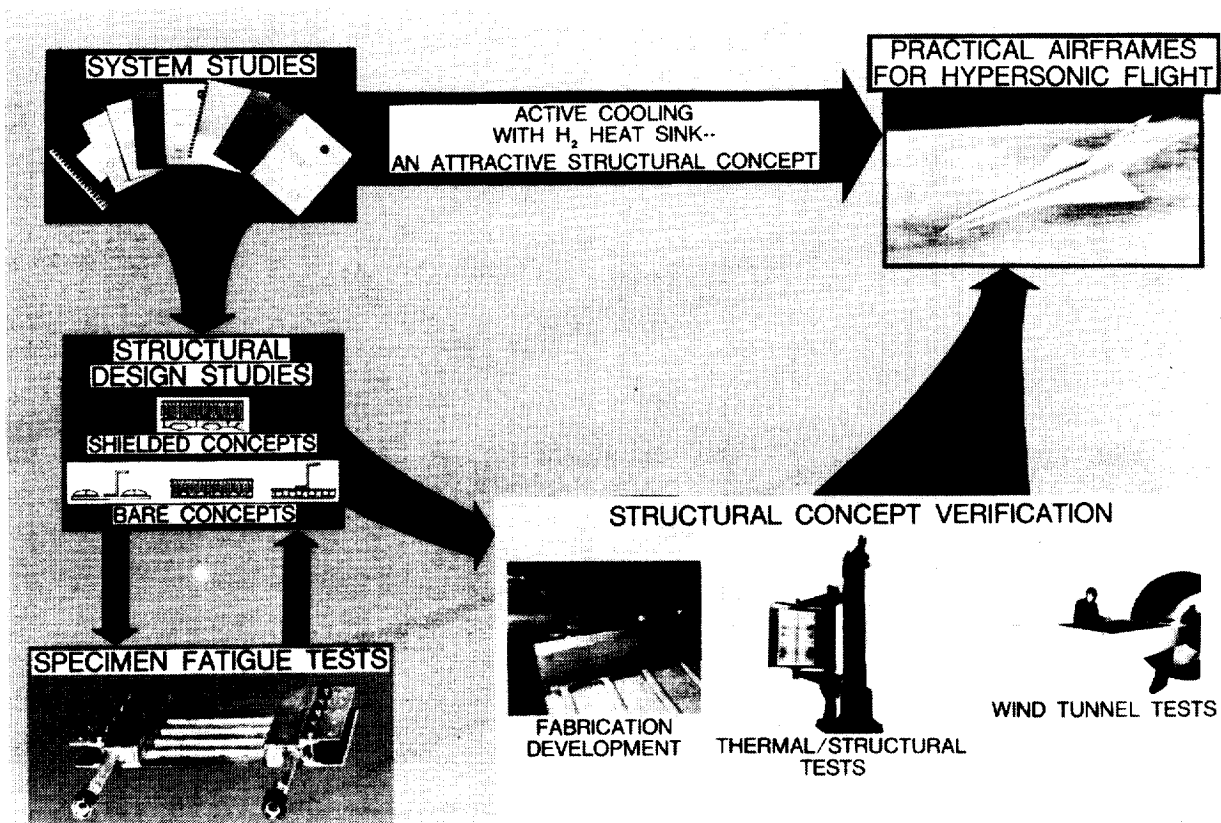


Figure 21

CONVECTIVELY COOLED CONCEPT SELECTION

Systems and hardware studies conducted in the mid 1970's yielded a coherent and consistent definition of the most attractive convectively cooled structural approach that combined both passive and active thermal protection. Recommended application regions for airframe concepts that combine passive and convective cooling are indicated in figure 22. Although the boundaries shown are specific to the constraints of the early studies, the trends are believed to have general applicability. At lower incident heat fluxes, an overcoated cooled structure is the favored concept. The overcoat, a moderate-temperature elastomeric material applied to the outer surface of the structure, is an outgrowth of the fail-safe abort studies described in reference 36. At higher heat fluxes the overcoat is replaced by high temperature insulation and heat shields. This approach represents a marriage of convective active cooling with the radiative heat shield technology developed for entry vehicles. Only at the highest heat flux levels where heat shields reach excessive temperatures would bare convectively cooled structures be used. Addition of a hot surface thermal protection to a bare convectively cooled structure reduces total mass, provides improved heat-load/heat-sink compatibility, increases safety and reliability, improves tolerance to off-design conditions, and eases fabrication difficulties.

APPLICATION REGIONS FOR CONVECTIVE/RADIATIVE COOLED AIRFRAME STRUCTURES

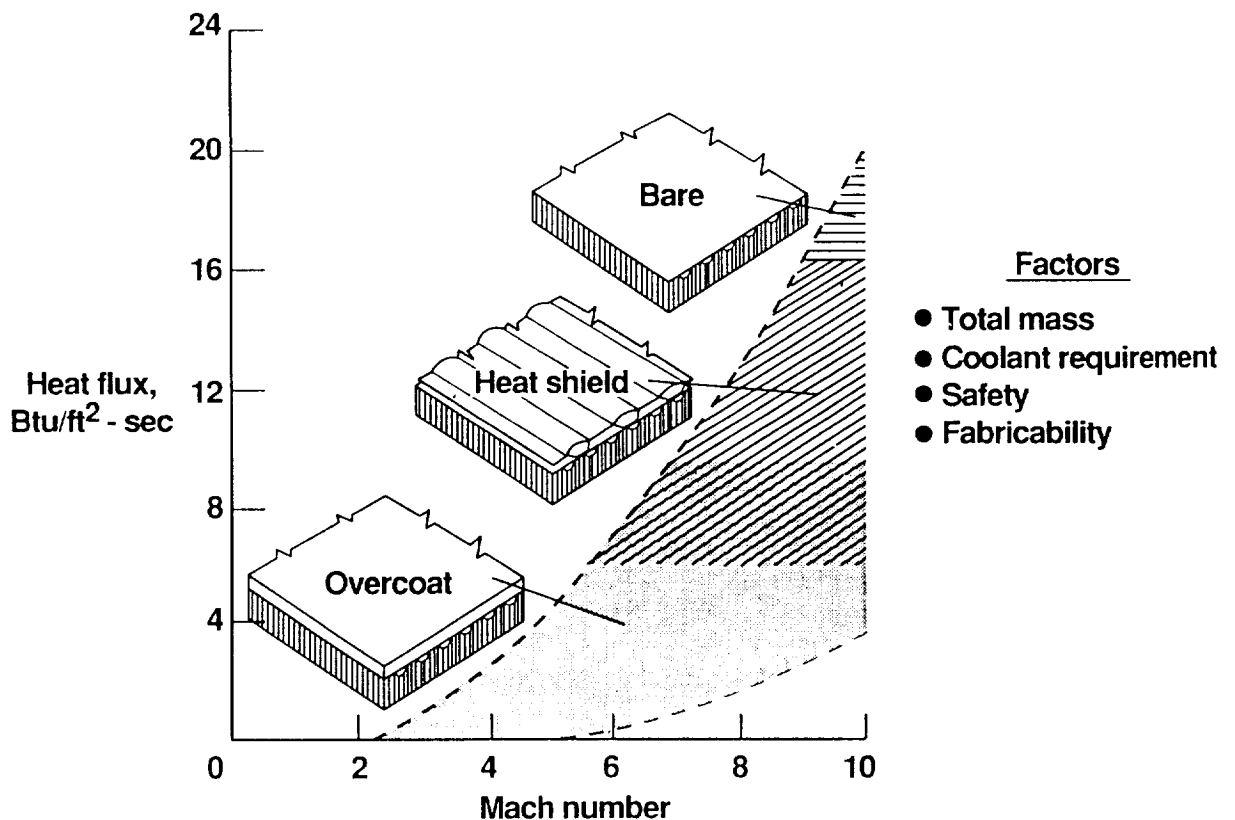


Figure 22

ACTIVELY COOLED PANEL PROGRAM - ALUMINUM CONCEPTS

To complement the system studies, a series of design and fabrication studies was undertaken to provide both bare and heat-shielded structural specimens for thermal-structural testing by NASA. Three bare concepts and one shielded concept were included in the studies. The full-scale 20-ft-long by 2-ft-wide panels were designed to meet Mach 6 to 8 transport requirements, to have 10,000 hours of life, and to survive 20,000 fully reversed limit load cycles. Each panel was designed to accommodate a heat flux of 12 Btu/ft²-sec, a uniform lateral load of 1 psi, and a uniaxial limit load of ± 1200 lb/in. The test panels were 4-ft-long segments of the full-scale panel.

The Bell Aerospace bare concept is a skin-stringer structure with dual (redundant) counterflow cooling passages, and uses glycol/water as a coolant (see lower right portion of figure 23). Coolant passages are quarter ellipse tubes with adjacent wire crack arresters adhesively bonded between a flat 0.032-inch-thick outer skin and a formed 0.020-inch-thick inner skin. The tubes contain the coolant pressure and eliminate peel stresses between the bonded skins. Both sets of cooling passages operate to maintain design temperatures during normal flight; should one of the redundant systems fail, either in the panel or distribution system, the panel has a life expectancy of 1/2 hour at normal operating conditions. The unit mass (includes panel, coolant inventory, pumping penalty, and coolant distribution system) for this concept is 4.25 lbm/ft².

The McDonnell Aircraft bare concept (not shown) has a single pass non-redundant cooling system (D-tubes) embedded in a honeycomb sandwich, which is designed to contain internal-coolant leaks. The coolant tubes are brazed to a manifold with double chambers to get full coolant flow along the transverse edge. The tube-manifold assembly is then soldered to the outer skin which forms one of the facesheets of the adhesively bonded honeycomb sandwich. Methanol/water is used as the coolant. The unit mass for this concept is 4.84 lbm/ft². Difficulties with the soldering process eventually led to abandonment of fabrication of the bare honeycomb sandwich concept. The heat shielded concept (shown in figure 23) is very similar to the bare honeycomb panel in that it uses small D-tubes and adhesively bonded honeycomb sandwich structure plus a layer of high temperature insulation and metallic heat shields. Since the insulation and corrugation stiffened Rene'41 heat shields operate at 1450°F, most of the incident heat is radiated away and the heat absorbed by the cooled panel is reduced by a factor of 10. As a result, the mass of the secondary cooling system is greatly reduced and the shielded concept has a unit mass of 4.52 lbm/ft² or 7 percent less than the corresponding bare concept. The much lower heat flux to the cooled panel permits use of adhesives to bond the cooling tubes to the outer face sheet rather than the soldering process needed for the bare panel.

The LaRC-Rockwell International concept (lower left of figure 23) uses a stringer-stiffened, brazed plate-fin sandwich (similar to hydrogen-cooled panels previously described for the HRE) with a rectangular-fin core for the main coolant passages. An auxiliary coolant passage outboard of the edge fasteners plus a thickened conduction plate provide longitudinal edge cooling. Stringers are adhesively bonded to the inner skin between frames. Glycol/water is used as the coolant. The unit mass for this concept is 4.46 lbm/ft².

References 20, 31, 32, 35, 37 and 38 discuss the design and fabrication of these actively cooled panels in more detail. Figure 23 is shown on next page.

ACTIVELY COOLED TEST PANELS

2- by 4-foot

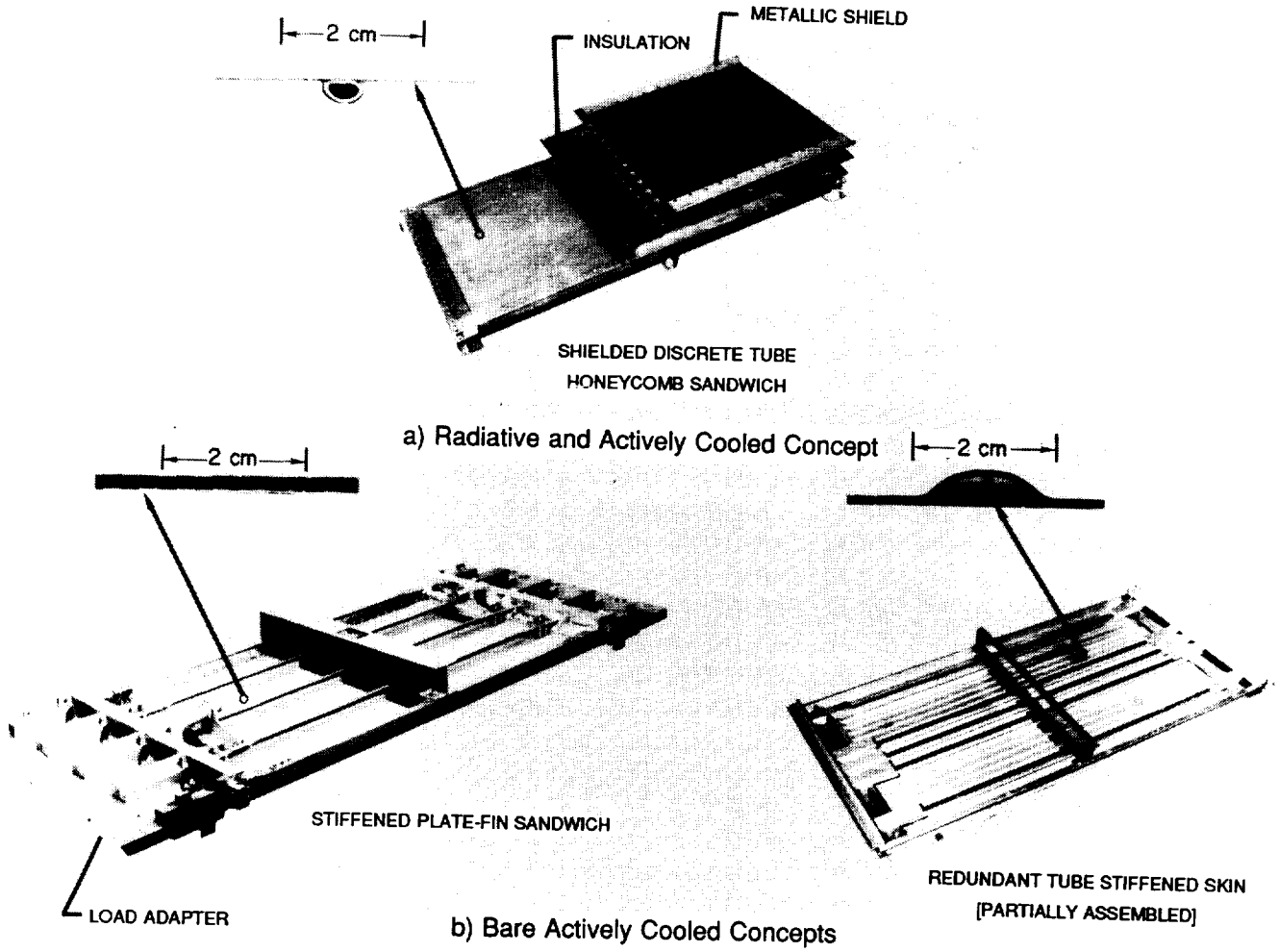


Figure 23

ACTIVELY COOLED HONEYCOMB SANDWICH AMBIENT TEMPERATURE FATIGUE TESTS

As part of the hardware design and fabrication studies, small specimens were fabricated and tested to determine fatigue life characteristics for each concept. Two of the bare honeycomb sandwich fatigue specimens are shown in figure 24. The upper specimen was used to check cooling-tube/facesheet characteristics and the lower specimen was used to check the assembled panel characteristics. Results from the fatigue tests indicated that: the fatigue life of 20,000 cycles was exceeded, the cooling tubes acted as crack arrestors for cracks induced in the facesheets, cracks in the facesheets which propagated past the coolant tubes did not penetrate into them, and leakage from cracks induced in the tubes was contained by the honeycomb sandwich. Finally, the tests also showed that there was a need to redesign the transverse joints to avoid excessive joint motion. Similar results were found for the transverse joints in the discrete tube concept and the plate fin concept, indicating that the need to cool the joints further complicates the difficult task of joint design.

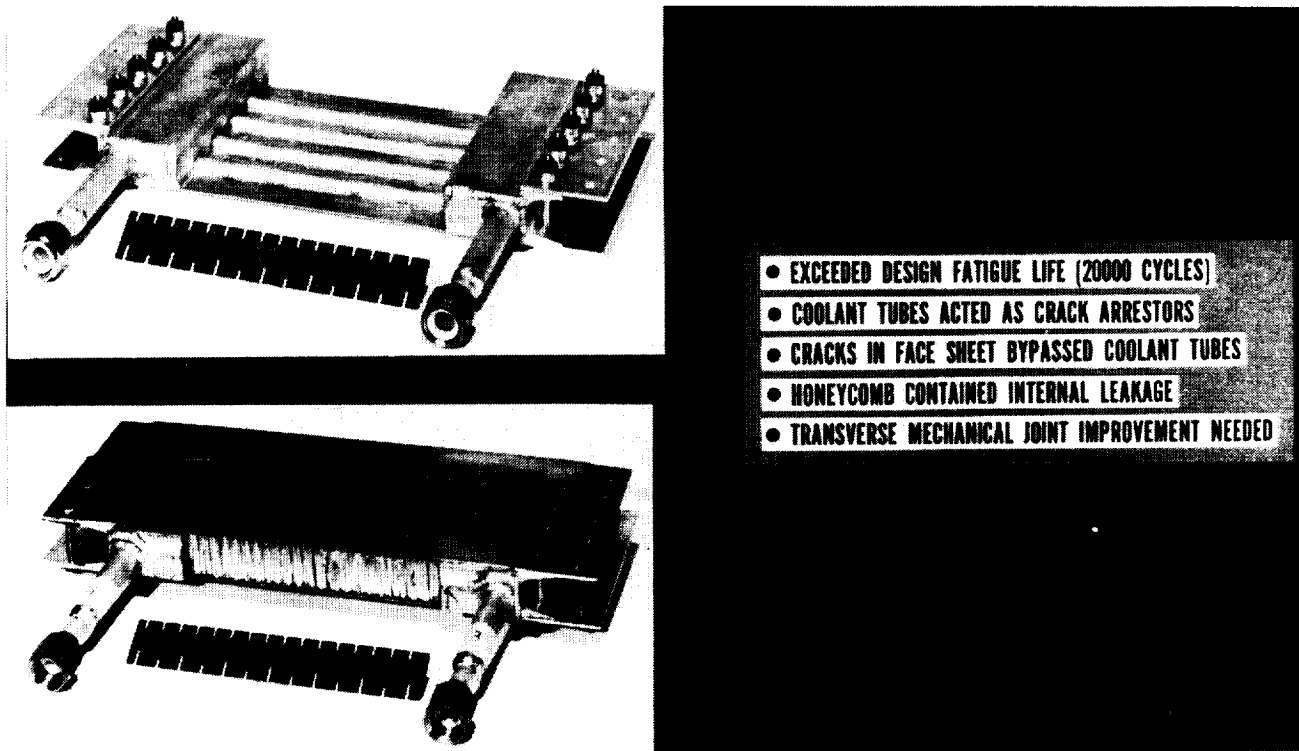


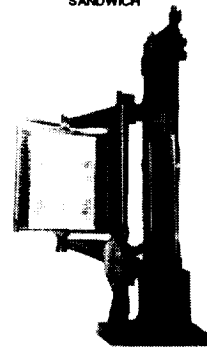
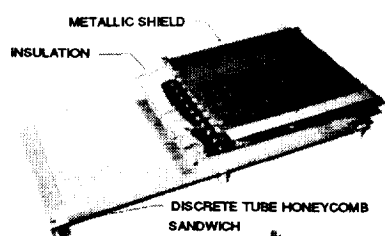
Figure 24

ORIGINAL PAGE
BLACK AND WHITE PHOTOGRAPH

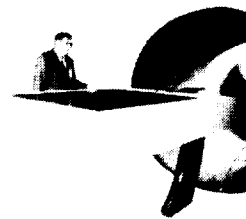
RADIANTLY AND ACTIVELY COOLED PANEL TEST RESULTS

As described in references 39 and 40 and shown in figure 25, the flight-weight heat-shielded convectively cooled panel was subjected to thermal-structural tests in the Active Cooling Test Stand (ACTS) shown at the bottom left of figure 25. The test represented design flight conditions for a Mach 6.7 transport and off-design conditions simulating flight maneuvers and cooling system failures. A total of 32 tests exposed the panel to 65 thermal cycles and multiple cycles of mechanical loading. The panel successfully withstood 55 hours of radiant heating at 12 Btu/ft²-sec, and 5000 cycles of uniaxial in-plane limit loading of ± 1200 lb/in. at operational temperatures. Additionally, the panel withstood off-design heating conditions for a simulated 2g maneuver from cruise conditions and simulated failures of the water/glycol cooling system without excessive temperatures on the structural panel. Wind tunnel tests in the Langley 8-Foot High Temperature Tunnel exposed the panel to 15 aerothermal cycles for a total of 137 seconds in a Mach 6.7 test stream. The panel responded as predicted and survived the extensive aerothermal and structural testing without significant damage to the structural panel, coolant leaks, or hot-gas ingress to the structural panel. However, the foil coverings on the insulation packages sustained damage sufficient to destroy their function of preventing water ingress to the layer of high-temperature insulation.

As an ancillary part of the investigation, a separate model of the heat shield was subjected to extensive thermal cycling (ref. 41). The 10.8-inch-wide by 23.9-inch-long model incorporated a mid-panel joint which was representative of the slip joint used in the full-scale design as were the other details of the heat shield. The heat shields survived exposure to 20,040 simulated flights (thermal cycles) and remained intact. However, a one percent shrinkage in the heat shield caused cracks and excessive wear to occur around the elongated fastener holes. Tensile tests of specimens machined from the heat shield showed an 80 percent loss in ductility and a 20 percent increase in yield strength compared to Rene'41 in the aged condition.



THERMAL/STRUCTURAL TESTS



WIND TUNNEL TESTS

- 55 HOURS AT DESIGN HEATING CONDITIONS
- 65 THERMAL CYCLES
- 5000 LOAD CYCLES AT TEMPERATURE
- THERMAL AND STRUCTURAL PERFORMANCE WITHIN 10-PERCENT OF PREDICTED PERFORMANCE
- 132 SECONDS [TOTAL] IN M = 7 AEROTHERMAL ENVIRONMENT
- WITHSTOOD SIMULATED ABORT [COOLANT LOSS] HEATING TRAJECTORY
- NO EVIDENCE OF HOT GAS INGRESS OR STRUCTURAL FAILURE OR COOLANT LEAKS

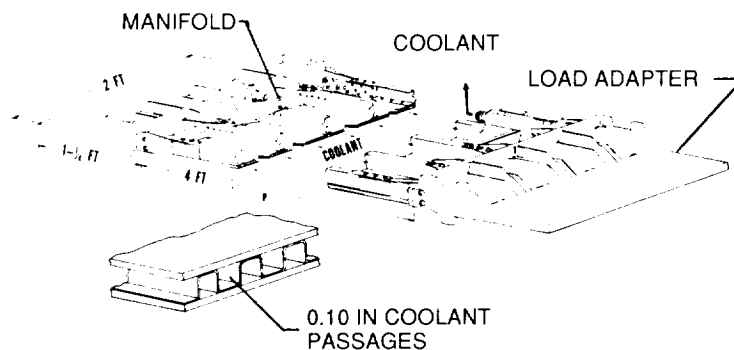
Figure 25

THERMAL-STRUCTURAL TESTS OF COOLED ALUMINUM PLATE/FIN PANEL

The LaRC-Rockwell glycol/water cooled aluminum structural panel (see figure 26) was tested under combined thermal and structural loading in the Active Cooling Test Stand shown in figure 25. More than 100 load cycles were applied at room temperature, and over 5000 load cycles were applied with the panel subjected to the design heat flux. The panel was subjected to 16 thermal cycles and more than 10 hours at elevated temperature. The maximum measured temperature was 231°F, and the maximum average heat flux was 11.8 Btu/ft²-sec. The coolant inlet temperature was varied from 48°F to 120°F in an attempt to simulate four-foot sections of the full scale 20-foot-long panel. The panel survived all of the testing with no evidence of structural damage. Visual and x-ray inspections indicated no cracking, and there were no significant changes in strain distribution during testing. Additional details of the investigation may be found in reference 42.

Several lessons were learned from this testing which will be even more important for testing of actively cooled structures at higher heat fluxes. (1) Sensors on the heated surface of an actively cooled structure encounter significant through-the-thickness temperature gradients, which must be factored into the data reduction. (2) Even for this high thermal conductivity aluminum panel, significant transient strains associated with thermal stress were observed during start up and shut down of the heaters. For lower conductivity materials subjected to higher heat fluxes, particular attention must be given to the thermal transients to avoid unrepresentative thermal stresses. (3) Because of entrance and transition effects in the coolant flow, thermal measurements from foreshortened coolant passages may not be representative of longer panels.

PANEL CONFIGURATION



TEST SUMMARY

HOT MECHANICAL LOAD CYCLES	5005
THERMAL CYCLES	16
TIME AT ELEVATED TEMPERATURE	10 HR 9 MIN
MAXIMUM MEASURED PANEL TEMPERATURE	231°F
MAXIMUM HEAT FLUX	11.8 BTU/(FT ² -SEC)
COOLANT INLET TEMPERATURE RANGE	48 TO 120°F

Figure 26

ACTIVE COOLING APPLICATIONS FOR NASP

The remainder of the present paper presents information taken from a review (ref. 6) of actively cooled structures development under the National Aero-Space Plane (NASP) project. Most of this work was performed under Work Breakdown Structure (WBS) elements 4.4.03 and 4.4.04 of the NASP Technology Maturation Program (TMP). Some additional information from the NASP Materials Consortium and the mainline engine program are also included. Details of the airframe studies (WBS elements 4.4.03 and 4.4.04) are presented in references 43 and 44.

Typical regions on NASP where active-cooling is required and the corresponding ascent conditions are indicated in figure 27. Fortunately for NASP, the most severe conditions occur during ascent when the cryogenic hydrogen fuel, which is an excellent coolant, is available as a heat sink. In many cases the more benign re-entry conditions dictate the maximum temperature requirements of the structure because the cryogenic fuel is not available as a coolant. The information presented in the present paper is limited to the acreage area applications (inlet ramp, nozzle, and engine interior), and is confined to convective cooling. Results of studies to develop cooled concepts for stagnation regions are described in references 45 and 46. Cooled airframe structures differ from engine structures in that, in addition to generally lower heat fluxes, the airframe structural loads are characteristically inplane loads. However, loads for engine structures arise primarily from the need to contain hot engine gases. Both engine and airframe structure must sustain thermal and coolant pressure loads.

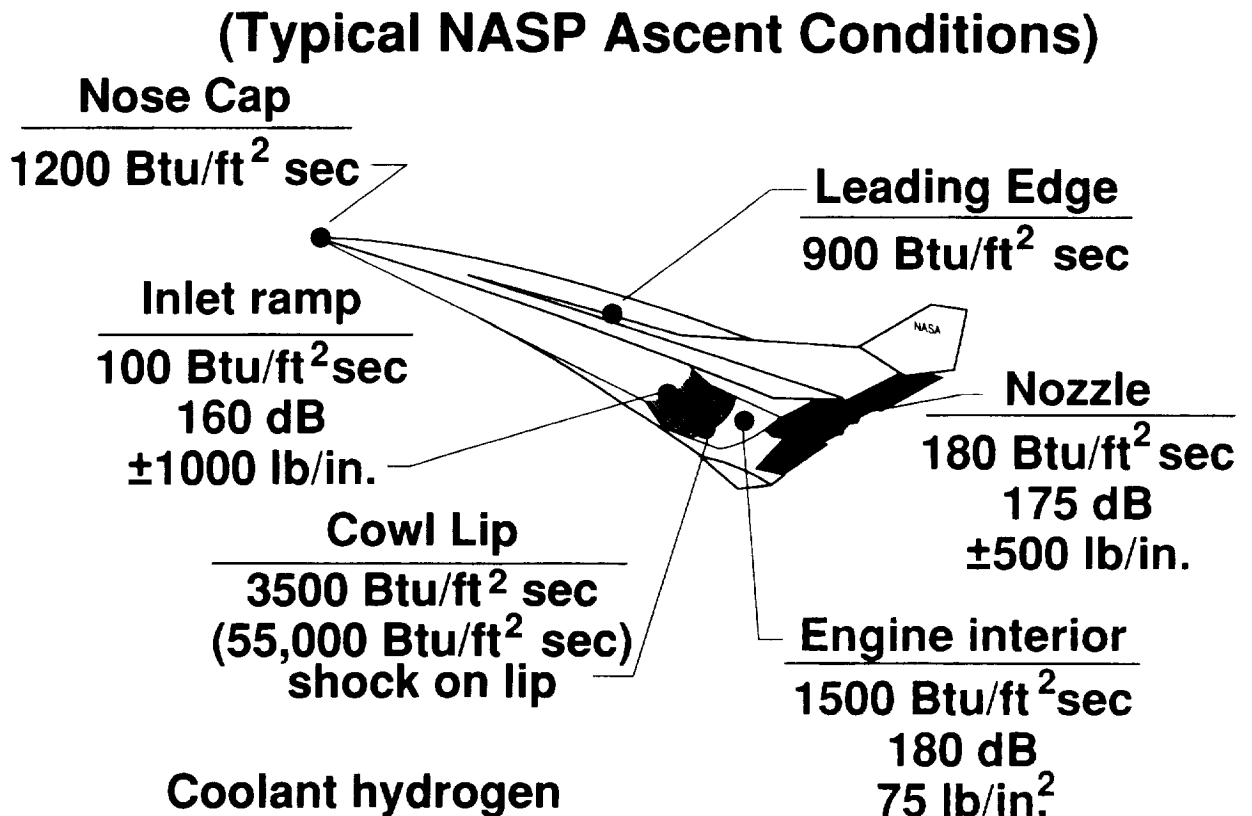


Figure 27

ACTIVELY COOLED PANELS MADE UNDER NASP TMP OPTION 3

The McDonnell Douglas Corporation NASP TMP Option 3 program (WBS 4.4.04) was conducted over a period of 5 years. Initial analytical studies included conceptual design and trade studies for inlet ramp, external nozzle, and control surface applications. Subsequent fabrication development efforts were limited to integral heat exchanger/structural concepts for the inlet ramp and non-integral heat exchanger/structural concepts for the nozzle. Several actively cooled panels were fabricated, two test facilities were constructed, checked-out and used to test the actively cooled panels. Details of the McDonnell Douglas work can be found in their TMP Option 3 Final report (ref. 44). Subcomponent (6 in. by 6 in.) and component (2 ft by 2 ft) panels fabricated at MDC's direction are shown in figure 28. The panels used a variety of materials (titanium metal matrix composite, beryllium, and copper/graphite), attachment concepts (integral and non-integral), and heat exchange configurations (D-groove and skin/tube). The subcomponent panels, which were part of the fabrication development, were tested at Wright Laboratories with gaseous nitrogen as a coolant. Subsequently the copper/graphite and beryllium platelet subcomponent panels and the full size component panels were tested in the hydrogen facility at WYLE Laboratories, Norco, California.

Details of the fabrication development and testing efforts are presented in references 47, 48 and 49.

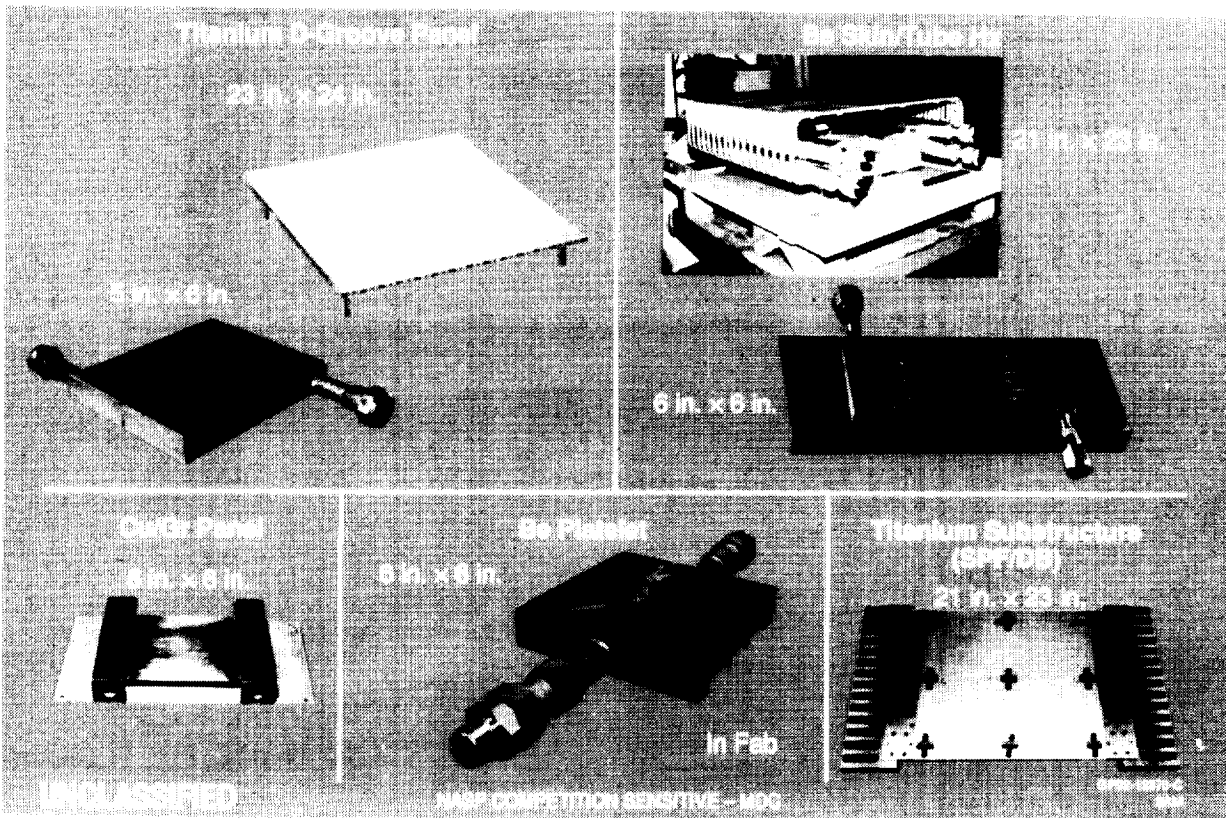


Figure 28

AFWAL SUBCOMPONENT PANEL TEST FACILITY

The Wright Laboratories (formerly AFWAL) active cooled thermal test facility provided the capability for testing of the subcomponent panels using room temperature N_2 as a coolant. The facility shown in figure 29 also incorporates a nitrogen tube trailer which is used to fill two 600 ft³ spheres. These spheres can be pressurized to approximately 4000 psi, which provides a reservoir for testing panels at pressures up to 2000 psi at flow rates on the order of 1 to 2 lb/sec. A graphite heater array provides heating rates up to 350 Btu/ft²-sec to the subcomponent panels. The test enclosure is also purged with nitrogen to protect the graphite heaters from oxidation. Additional details of the facility may be found in references 44 and 50.

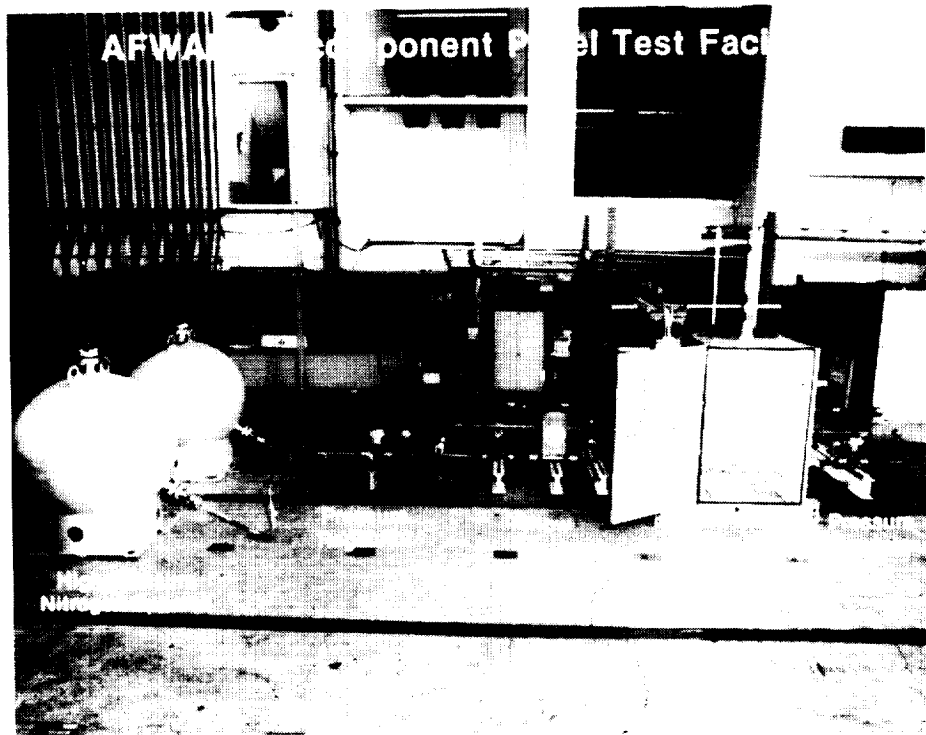


Figure 29

ORIGINAL PAGE
BLACK AND WHITE PHOTOGRAPH

WYLE LABORATORIES H₂ ACTIVE COOLING TEST FACILITY

A thermal/structural facility for testing actively cooled panels (see figure 30) was established at the WYLE, Norco test site. This facility, which can accommodate panels up to 2-ft by 4-ft, uses nitrogen or supercritical hydrogen as coolants. Hydrogen can be provided at temperatures between -360°F and +40°F, flow rates up to 2.3 lb/sec, and pressures up to 2000 psi. Heating capability extends up to approximate 280 Btu/ft²-sec. Additionally, the facility is capable of providing mechanical loads (either tension or compression) of up to 48,000 lbs. The test chamber is continuously purged with N₂ to protect and extend the life of the graphite heaters. Additional details of the facility are presented in references 44, 49 and 51.

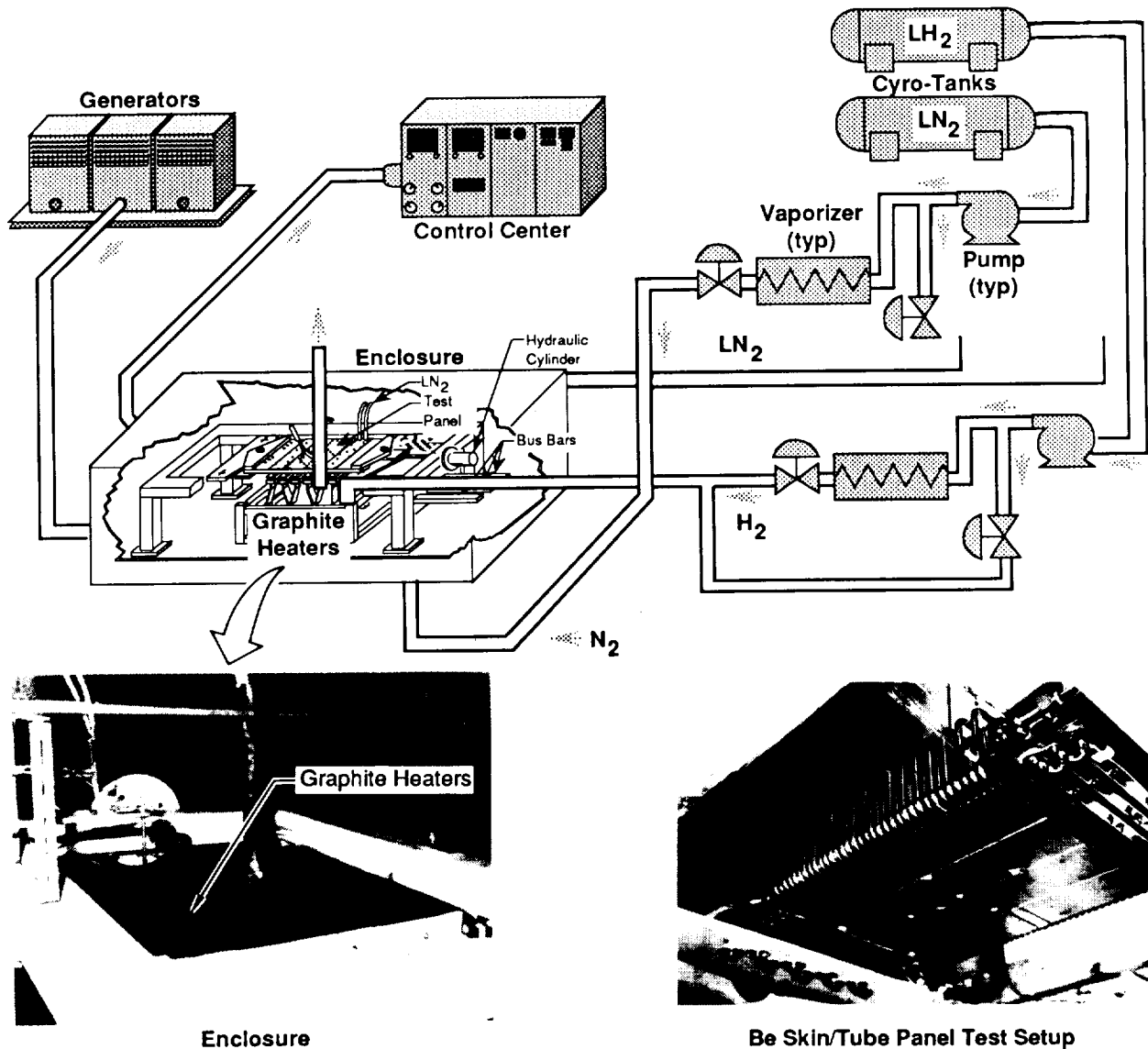


Figure 30

THIS PAGE
BLACK AND WHITE PHOTOGRAPH

TITANIUM D-GROOVE PANEL

The titanium D-Groove panel (see figure 31) which was designed for an inlet ramp for NASP is representative of an integral heat exchanger/structural design in that the heat exchanger and substructure are metallurgically bonded to form a single entity. The panel was designed by McDonnell Douglas Corporation and fabricated by Rohr Industries. The materials of construction for this panel were the best high temperature titanium alloys currently available.

The panel materials are given below:

outer face sheet	•	SiC/Ti*
etched sheet	•	Ti-14Al-21Nb
honeycomb	•	Ti-15V-3Cr-3Sn-3Al
manifold/edge	•	Ti-6Al-2Sn-4Zr-2Mo
inner face sheet	•	SiC/Ti*

The design chosen extends the coolant passage as close to the edges as possible by folding the flow back on itself as it exits the manifold and enters the D-shaped coolant passages. This is done to prevent overheating of the panel-to-panel joint region. The manifolds also form the load path through which in-plane mechanical loads are transmitted from panel to panel.

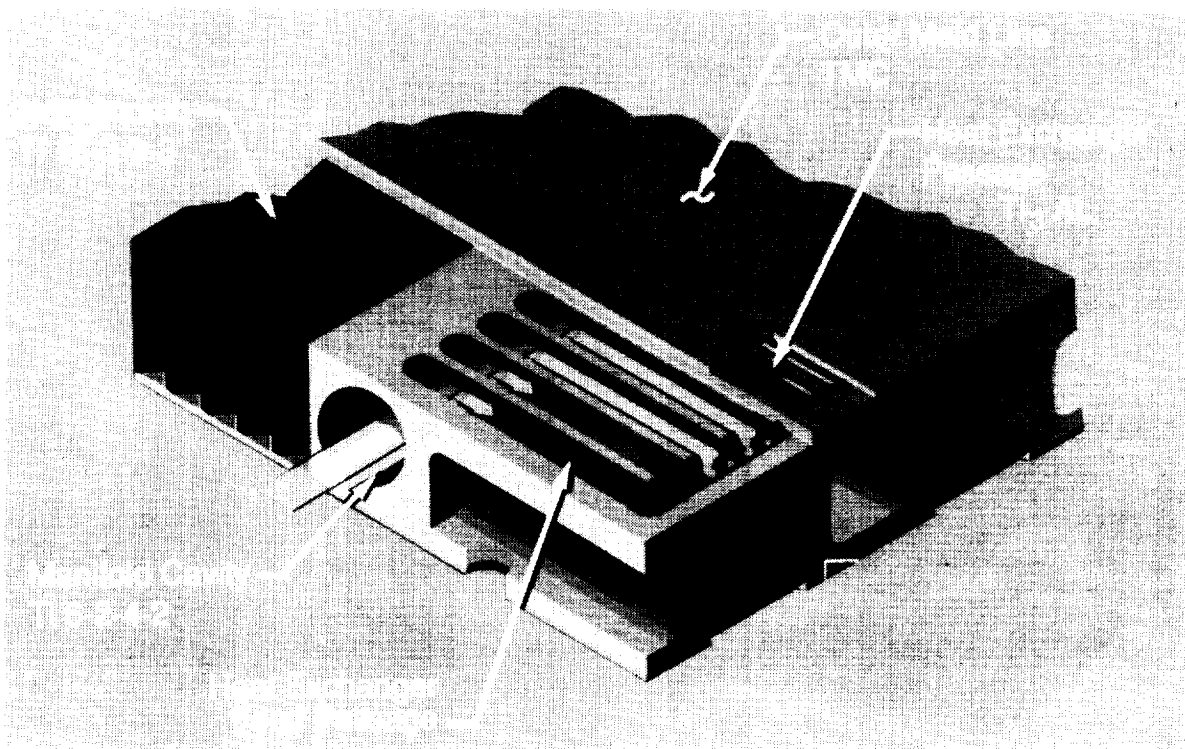


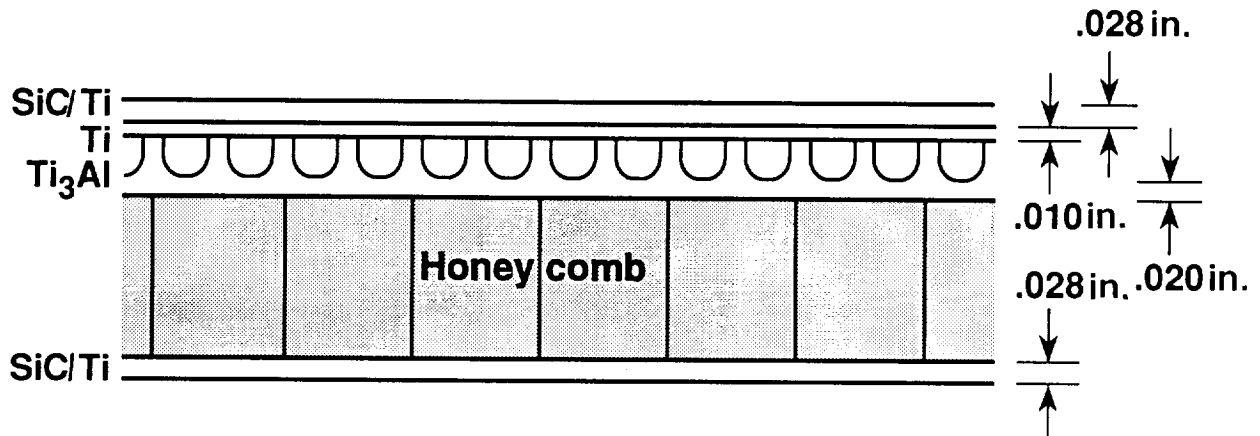
Figure 31

* The outer and inner facesheets are titanium matrix composites (TMC) comprised of 0.0056 in. diameter silicon carbide fibers (SCS-6) in a Ti-15V-3Cr-3Sn-3Al matrix.

TITANIUM D-GROOVE PANEL FAILURE

The 2-ft by 2-ft Titanium D-groove panel which had been hydrostatically tested previously to 3000 psi failed without warning at a pressure of approximately 1/10 that value as the panel was being pre-cooled with nitrogen prior to testing. Design and test conditions for the titanium D-groove at failure are summarized in figure 32. Exact conditions at failure are unknown since the data acquisition system had been deactivated, after the panel had been at approximately the indicated conditions for about one hour while malfunctioning test equipment was being repaired.

SiC Ti - Ti₃ Al GROOVED PANEL



- Design: 100 Btu/ft²sec, 1000 lb/in., 2000 psi LH₂ coolant
- Failed: Prior to test, during panel precooling with N₂
- Conditions: 0 Btu/ft²sec, 0 lb/in., 340 psi N₂ @ 20-40°F
- Residual stress 55 ksi; critical crack length 0.040 in.

Figure 32

HEAT EXCHANGER SKIN FRACTURE

The nature of the damage to the failed Titanium D-groove panel is shown in figure 33 (note that the photograph in the lower left corner of figure 33 shows load adaptors and carrying frame that are not part of the panel). While the exact cause of failure was not ascertained, it is believed that poor fracture toughness (as evidenced by the small critical crack length), residual stresses (because of the mismatch in thermal expansion characteristics of the cover and grooved sheets), and one or more flaws in the titanium aluminide grooved sheet were involved. The failure mechanism postulated from the post-test analysis suggests the following scenario: 1) a failure, quite possibly an overload or crack growth failure in the grooved titanium aluminide sheet, opened the honeycomb cavity to high pressure nitrogen; 2) since the honeycomb was not perforated, the honeycomb cells failed progressively at the braze joint with the top and bottom face sheets; 3) after a large enough area of the honeycomb had been disbonded from the skin, the internal pressure became large enough to rupture the skin (refs. 44 and 49).

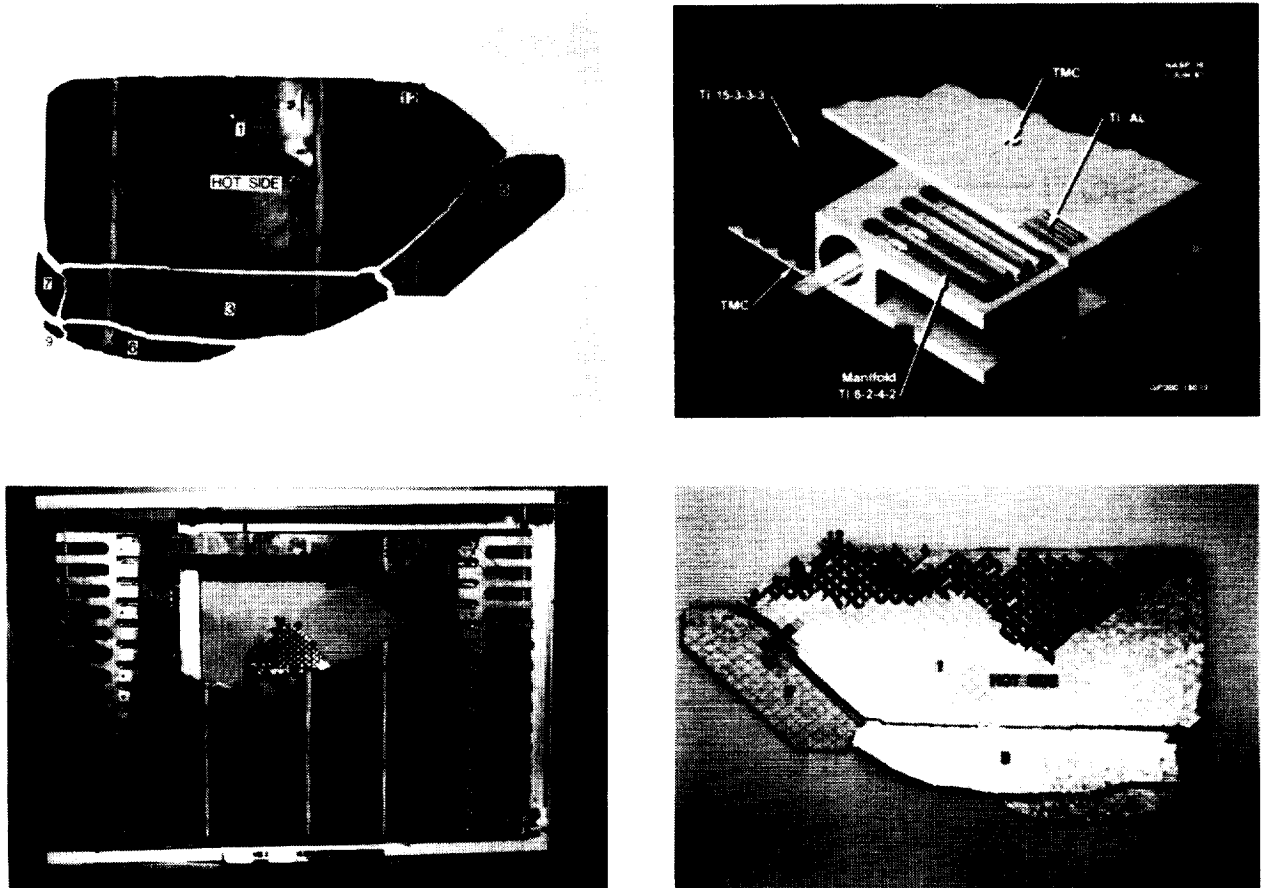


Figure 33

BERYLLIUM SKIN/TUBE PANEL

Figure 34 illustrates the conceptual design of an actively cooled panel for an exterior nozzle application as viewed from the back side. This concept employs a non-integral beryllium skin/tube heat exchanger mounted onto a four sheet titanium superplastically formed/diffusion-bonded (SPF/DB) sandwich structure by means of nine slide mechanisms which allow for differential thermal expansion between the heat exchanger and the titanium sub-structure. This panel concept which was chosen to demonstrate the efficient utilization of high-thermal-conductivity materials, features counter flowing coolant in adjacent coolant passages. Manifolds supplying coolant to the heat exchanger, which were not a flight-weight design, were of stainless steel. The design was developed by McDonnell Douglas Corporation and fabricated by Electrofusion Corporation.

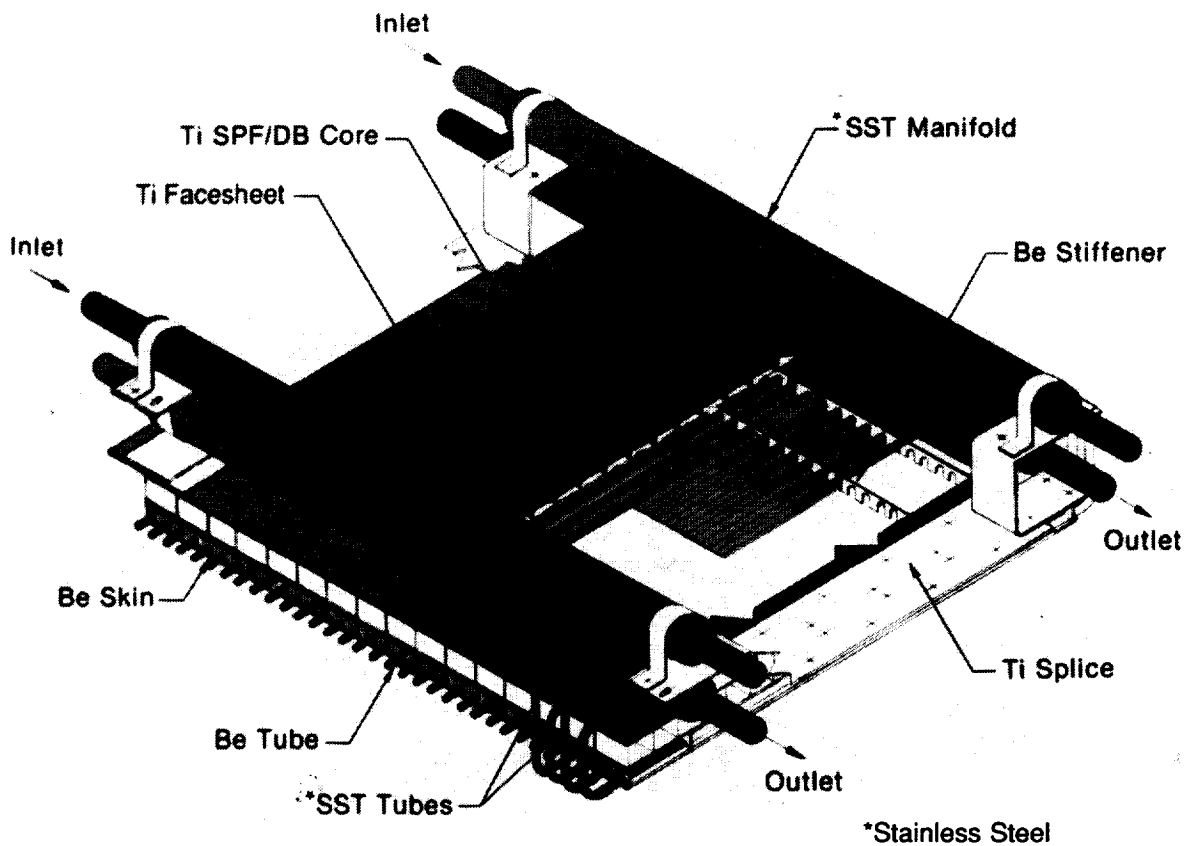


Figure 34

BERYLLIUM SKIN/TUBE PANEL MOUNTED IN WYLE TEST FACILITY

Figure 35 shows the heated surface of the beryllium skin/tube panel mounted in the WYLE load frame prior to testing. Part of the load fitting is visible at the left end of the panel. Also visible at both ends are copper heat exchangers which were used to maintain the load fittings at or near the same temperature as the titanium substructure. For actual testing a graphite heater array was mounted beneath the panel and the panel and heater were enclosed within a ceramic box to limit heat loss.

During initial testing the panel was exposed to eight heating periods of various intensity totaling 2.4 hours and reached a maximum heat flux of approximately 70 Btu/ft²-sec using hydrogen (at temperatures down to -90°F) as the coolant. Instrumentation difficulties occurred and all hot surface sensors were destroyed. The remaining thermal measurements agreed well with predictions; however, the strain measurements were less reliable. For more details, see references 44 and 49.

HEATED SIDE

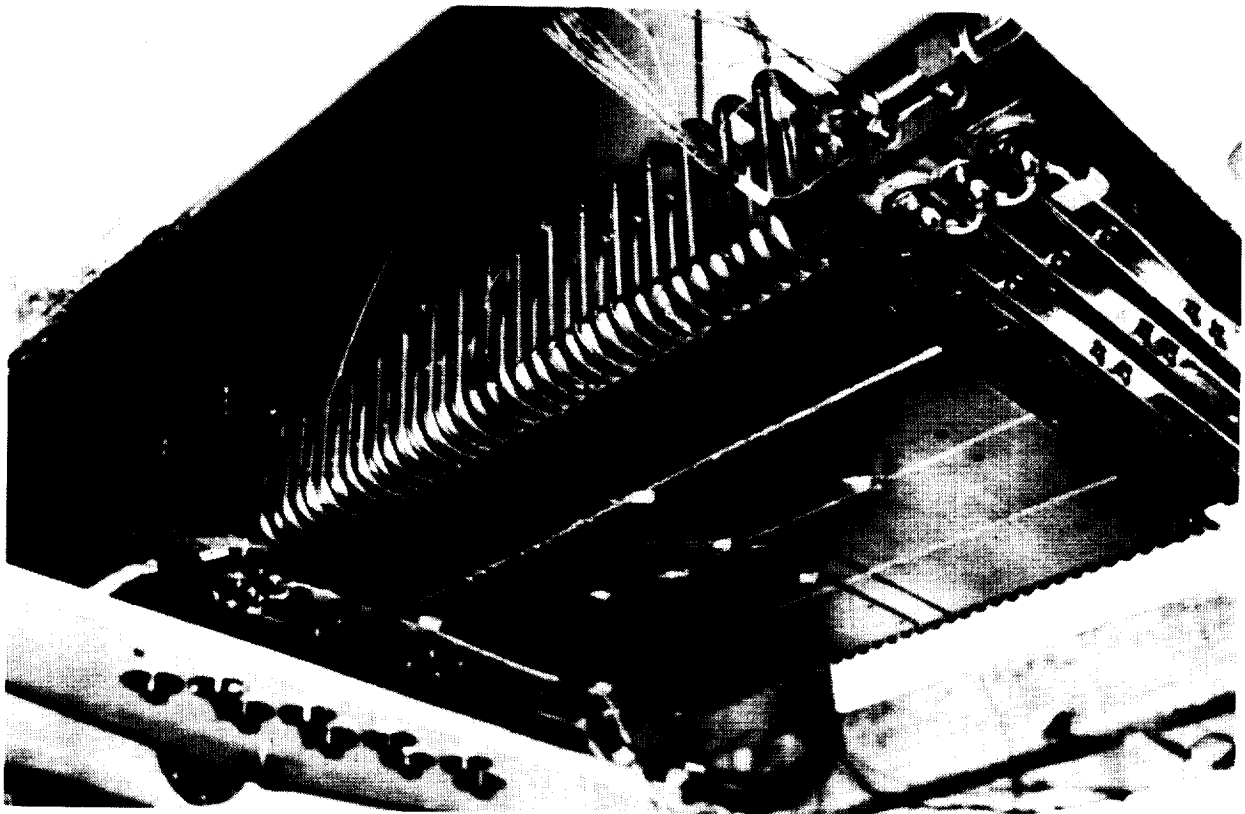


Figure 35

ORIGINAL PAGE
BLACK AND WHITE PHOTOGRAPH

BERYLLIUM SKIN/TUBE PANEL SHATTERED DURING FAILURE

After the successful tests at 70 Btu/ft²-sec, the skin/tube panel failed catastrophically under essentially no load as the coolant inlet temperature was being lowered from -90°F to -150°F. The panel at the time of failure was at a temperature of approximately -126°F, contained cryogenic hydrogen at a pressure of 1600-1800 psi, and was exposed to a heating rate less than 1 Btu/ft²-sec. The panel had previously been hydrostatically tested to 3000 psi at ambient temperature. As indicated by figure 36 the beryllium heat exchanger surface was completely blown away, exposing the titanium structural subpanel which was undamaged. The entire beryllium panel actually shattered into thumbnail-size pieces.

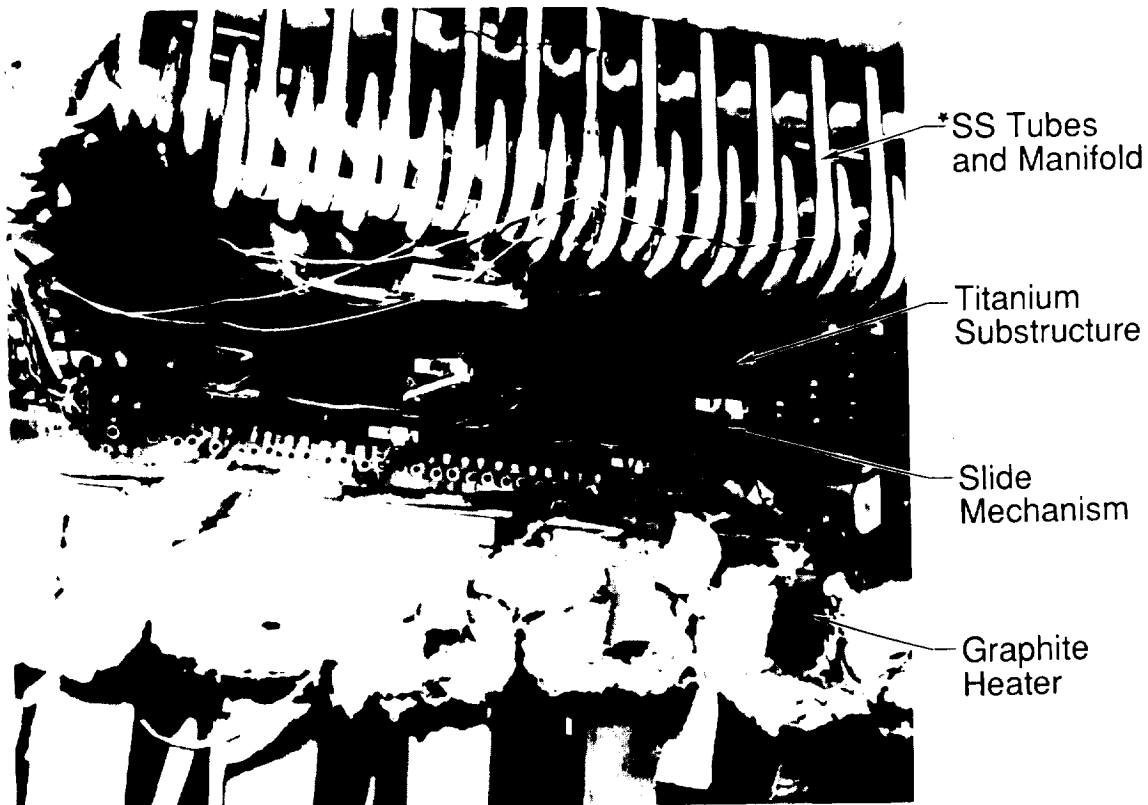


Figure 36

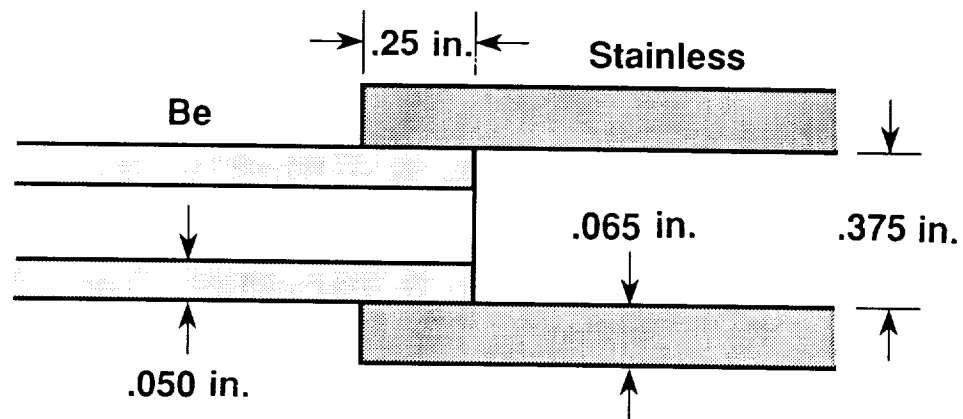
*Stainless Steel

ORIGINAL PAGE
BLACK AND WHITE PHOTOGRAPH

BERYLLIUM TUBE-SKIN PANEL

Design and test conditions at failure are summarized in figure 37. Large compressive circumferential stresses are induced in the beryllium tube by the stainless steel tube as the temperature of the joint decreases from the braze consolidation temperature of approximately 1000°F to the failure temperature of -126°F. This compression of the beryllium tube by the surrounding stainless steel tube also induces large axial bending stresses in the beryllium tube at the joint. These large axial tensile stresses, resulting from bending, exceed the strength capabilities of the beryllium at the failure temperature.

An extensive failure analysis concluded that a mismatch in thermal expansion characteristics of a dissimilar metal (beryllium-stainless steel) brazed tube joints in the coolant manifolds was the most probable cause of failure. As stated in reference 52, "Localized high stresses, resulting from brazing (together) materials having different coefficients of thermal expansion, initiated a brittle fracture of one or more beryllium tubes . . . (which) led to a rapid progressive break-up of the panel." (Note that the beryllium-stainless steel tube joint was an artifact of the test configuration and was not subjected to thermal stress analysis before testing.)



- Design: 160 Btu/ft²sec, 500 lb/in., 2000 psi LH₂ coolant
- Failed: As coolant temp being lowered from -90° to -150°F after a successful 70 Btu/ft²sec test
- Thermal stress: Be/347 stainless steel tube joint
 - Circumferential (under/joint) -61 ksi
 - Meridional bending (edge of joint) +58 ksi

Figure 37

BERYLLIUM PLATELET COMPONENTS

A subcomponent beryllium panel was fabricated as part of the NASP TMP Option 3 actively cooled panel activity. The design was developed by Aerojet TechSystems and McDonnell Douglas Corporation and the panel was fabricated by the Electrofusion Corporation. The panel construction details are shown in figure 38. A series of 55 D-shaped grooves were chemically milled into a .07-inch-thick beryllium plate. An orifice was electric discharge machined (EDM'd) into the end of each channel. A .030-inch-thick close-out sheet was brazed to the chemically milled plate. A variable area manifold was then brazed to each end of the heat exchanger panel, along with a beryllium egg-crate structure. Manifold inlet and outlet tubes (not shown in the photograph) were brazed to the manifold. Originally these tubes had a beryllium-stainless steel braze joint similar to the beryllium skin/tube manifold joints. Subsequently the stainless steel tubes were replaced with Inconel 718 tubes to avoid the coefficient of thermal expansion mismatch problem experienced with the beryllium skin/tube panel.

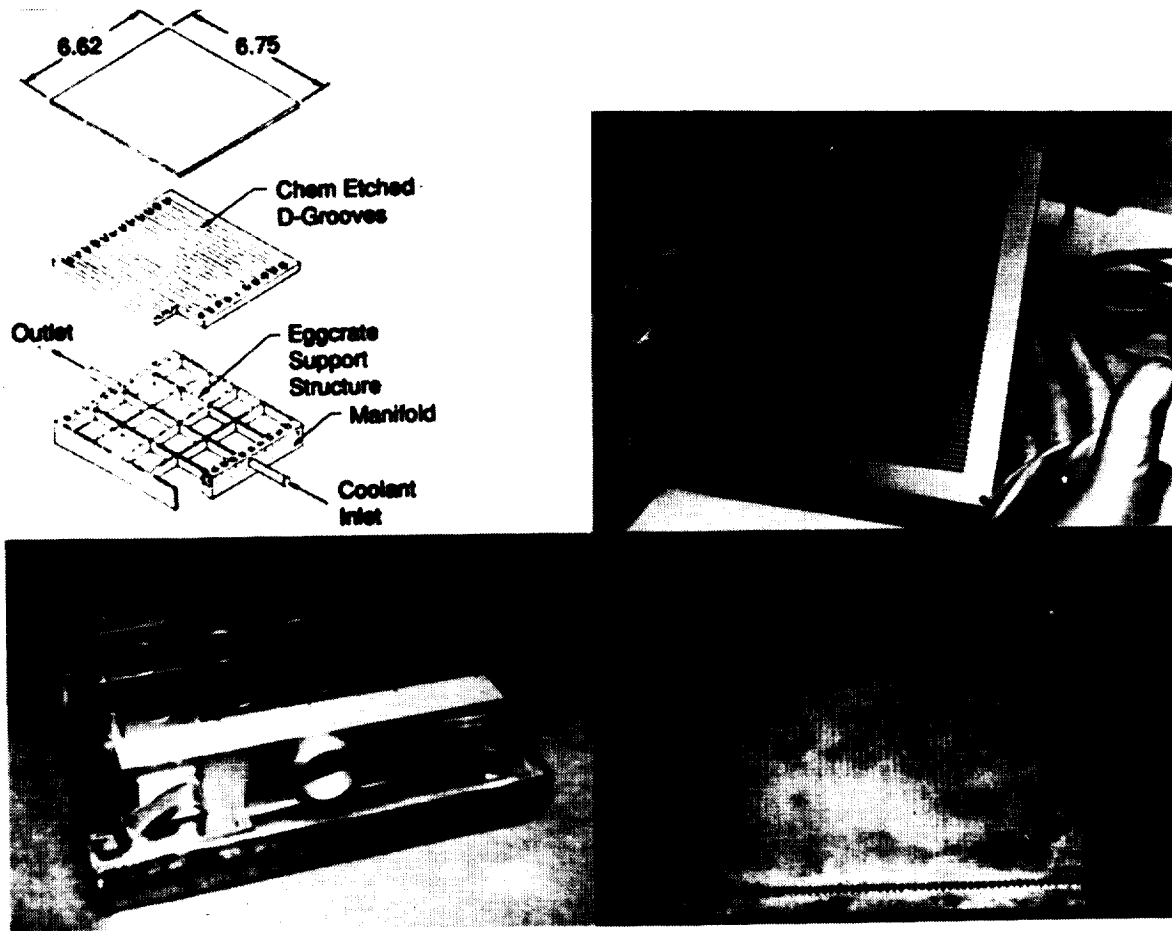


Figure 38

BERYLLIUM PLATELET PANEL TEST SUMMARY

The table in figure 39 summarizes the beryllium platelet panel tests at both Wright Laboratories and Wyle Laboratories. The panel as originally fabricated was tested at Wright Laboratories with gaseous nitrogen as the coolant. This panel had beryllium/stainless steel tube joints similar to those which failed in the beryllium tube-skin panel tests described previously. However, minimum temperatures encountered were approximately 40°F, which is well above the temperature at which the beryllium skin-tube panel failed. (Note that lower temperatures produce higher thermal stresses in the beryllium-stainless steel tube joint.) The panel was tested at various heating rates up to the maximum attainable with the graphite heater (280 Btu/ft²-sec) and exposed to 34 thermal cycles with heat fluxes of 200 or greater with no evidence of damage. Before testing with hydrogen coolant at significantly lower temperatures, the panel was modified to eliminate the beryllium-to-stainless-steel tube joint, as described previously. The modified panel was tested at WYLE laboratories with supercritical H₂ as the panel coolant at inlet temperatures as low as -200°F and heat fluxes as high as 280 Btu/ft²-sec. Subsequently the panel was exposed to an additional 98 thermal cycles at heat fluxes up to 200 Btu/ft²-sec with no evidence of damage. Post-test thermal analysis has produced very close agreement with measured test data. Further details are given in reference 44.

WRDC FACILITY TESTS

Heat Flux (Btu/ft ² - sec)	Flow Rate (lb/sec)	Coolant	Inlet Temperature (°F)	Inlet Pressure (psi)
50	1.5	N ₂	30	2000
100	1.5	N ₂	30	2000
150	2.5	N ₂	30	2000
200	2.3	N ₂	30	2000
250	2.3	N ₂	30	2000
280	2.3	N ₂	30	2000
200	0.8	N ₂	30	2000
200 30 Thermal Cycles	1.4	N ₂	30	2000

WYLE LABORATORIES TESTS

0-280 ↓ ↓ ↓	0.1-0.2	H ₂	40	2000
	0.1-0.2	H ₂	-70	2000
	0.1-0.2	H ₂	-140	2000
	0.1-0.2	H ₂	-200	2000
0-200 98 Thermal Cycles	0.1-0.2	H ₂	-70	2000

Figure 39

COPPER/GRAPHITE SUBCOMPONENT PANEL

A cross-section of the Cu/Gr panel fabricated by Sparta Incorporated under the McDonnell Douglas Corporation (MDC) Option-3 contract is illustrated in figure 40, together with the final assembled hardware. The Cu/Gr panel is made from two mated symmetric, grooved half panels. Each half panel uses a symmetric ply layup consisting of an outer copper foil layer, two plies of Cu/Gr (90° fiber orientation) and three plies of Cu/Gr with fibers in the 0° orientation. The cross-ply design increases the panel strength in the two orthogonal directions. Fifty-six nickel tubes, embedded within the two half sheets, serve to limit the diffusion of hydrogen into the Cu/Gr composite. The 6-inch square panel was part of the fabrication development and is equipped with non-flight type manifolds. Details of the design and fabrication are presented in reference 53.

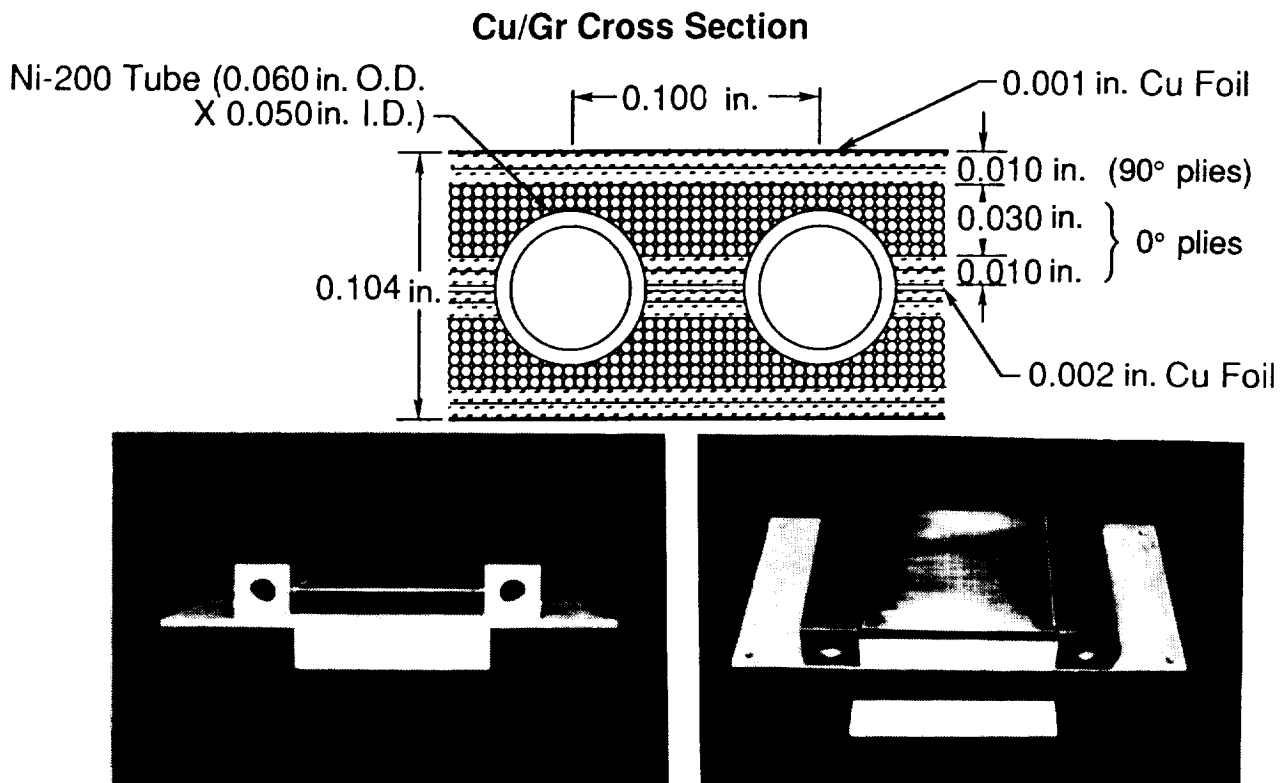


Figure 40

Cu/Gr SUBCOMPONENT PANEL TEST SUMMARY

The table shown in figure 41 summarizes the Cu/Gr panel tests at Wright Laboratories. Handling of the Cu/Gr panel prior to the tests resulted in several cracks in the bare nickel tubes immediately adjacent to the manifolds. As a consequence, the inlet N₂ pressure was limited to 1500 psi to minimize the impact of tube leakage. The panel successfully survived 50 thermal cycles at a heat flux of 200 Btu/ft²-sec and a maximum heat flux of 350 Btu/ft²-sec. However, as in all other tests, hot surface instrumentation failed at a heat flux of 98 Btu/ft²-sec or less. Trends indicated by the temperatures measured by back side thermocouples were similar to those predicted analytically; although the measured temperatures were consistently higher.

Subsequent to the tests at Wright Laboratories, copper was electroplated over the exposed tubes in an attempt to repair the leaks. These repairs were partially successful. Attempts to test the Cu/Gr panel with hydrogen at the Wyle test site were aborted because of the highly non-uniform thermal response of the panel. Post-test examination revealed that seven of the tubes at the far end of the inlet manifold were either totally or partially blocked by debris. These results emphasize the need for cleanliness when small coolant passages are involved. Additional information is presented in reference 44.

Heat Flux (Btu/ft ² - sec.)	Flow Rate (lb/sec)	Coolant	Inlet Temperature (°F)	Inlet Pressure (psi)
50	0.5-1.3	N ₂	30	1500
98	0.5	N ₂	30	1500
150	1.0	N ₂	30	1500
200	1.0	N ₂	30	1500
250	1.0	N ₂	30	1500
300	1.0	N ₂	30	1500
350	1.5	N ₂	30	1500
200 50 Thermal Cycles	0.4-1.0	N ₂	30	1500

Figure 41

Cu/Gr ACTIVELY COOLED PANEL

After some initial generic studies, the Rockwell actively cooled primary structure program (NASP TMP WBS 4.4.03) was focused on concepts suitable for the engine structure. An advanced copper graphite (Cu/Gr) design concept, similar to that developed under WBS 4.4.04, was selected for the diffuser and film cooling was selected for the combustor.

The heat exchanger for the diffuser panel (see figure 42) is integrally bonded to the support structure. The heat exchanger is made of cross-plyed Cu/Gr material with embedded Ni 200 coolant passages. The tubes are 0.005-in. thick and have an outer diameter of 0.060 in. The heat exchanger and honeycomb thicknesses are 0.104 in. and 1.0 in., respectively. The graphite fiber is P-130X, which has a thermal conductivity three times that of copper at room temperature.

The design loadings are heat flux = 800 Btu/ft²-sec, coolant pressure = 2000 psi, and aerodynamic pressure = 10 psi. Supporting analyses have been performed using the design conditions. These analyses show low thermal gradients in the heat exchanger and acceptable stresses in the Cu/Gr material. Classical lamination theory, three-dimensional, two-dimensional, and metal-matrix composite codes, were used in the analyses.

Three small heat exchanger fabrication articles were fabricated with each measuring 2 in. by 6 in. One of these articles was cut into 1 inch square pieces for thermal cycling tests. These tests were performed from cryogenic (-250°F) to elevated (800°, 1000°, and 2000°F) temperatures for 1, 5, and 50 cycles. It was concluded that the material and design were capable of a 1000°F operating temperature, although more testing is necessary.

Two 12 in. by 12 in. Cu/Gr actively cooled panels have been fabricated by SPARTA Incorporated (reference 53). Thermal testing will be performed in the Rocketdyne Materials Structural Thermal Validator (MSTV-1) shown in figure 43. Characterization tests will determine the effect of coolant pressure, flow rate, and heat flux variations. Thermal cycling will be performed by varying an applied heat flux between 200 and 800 Btu/ft²-sec to demonstrate cyclic life. Acoustic testing will be performed in a plane wave facility at the Rockwell North American facility to a maximum level of 168 db. To determine panel response at the higher engine environment, the panel can be characterized by vibration testing. These results can be superimposed onto the acoustic test results. Fatigue testing of heat-exchanger/honeycomb articles will be performed to determine the acoustic fatigue behavior of the design. Additional details of the Rockwell studies may be found in reference 43.

(Figure 42 is shown on the next page.)

Gr/Cu Actively Cooled Panel

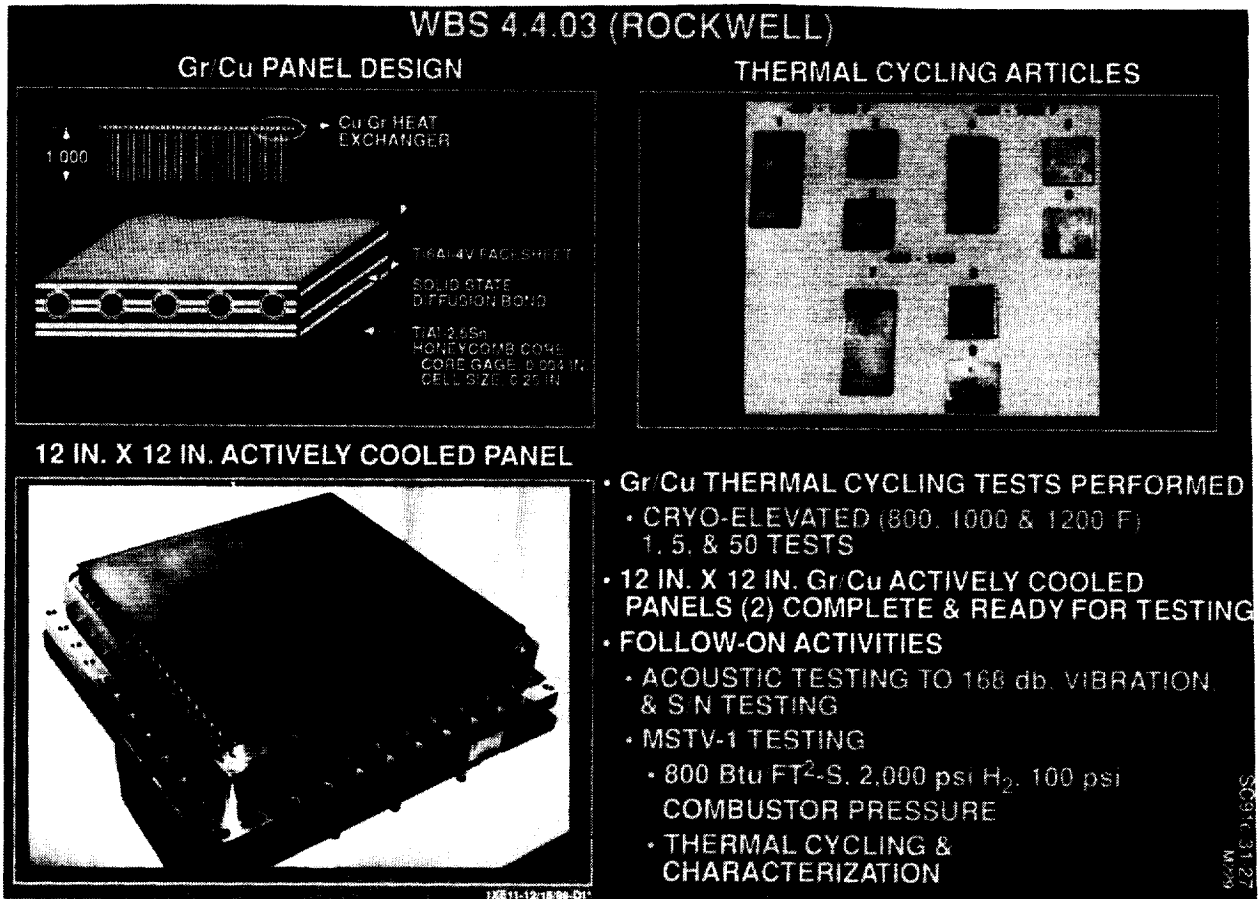


Figure 42

MATERIALS STRUCTURAL THERMAL VALIDATOR (MSTV-1) TEST RIG

The MSTV-1 test rig is a rectangular two dimensional hot gas generator, which burns liquid oxygen and gaseous hydrogen. The products of combustion, which will reach temperatures up to 6000°R, will be used to test actively cooled panels, attachments, seals and substructures. Fabrication of the MSTV-1 is complete and the test rig is currently being calibrated. The MSTV-1, shown in figure 43, is designed to supply a surface heat flux of 350 to 1400 Btu/ft²-sec with a chamber pressure of 65 to 350 psi, to a 12 in. by 12 in. actively cooled panel. The rig can operate from 30 to 50 seconds at maximum heat flux. Hydrogen coolant can be supplied to the panel test rig at a maximum rate of 2 lb/sec and an inlet pressure of 2670 psi at room temperature. An additional supply of 200°R hydrogen is also available. Real time calorimetry during the test of an actively cooled panel can also be provided. Tests of NARloy Z and Incoloy 909 cooled panels, attachments, seals and substructures are planned as part of the NASP program.

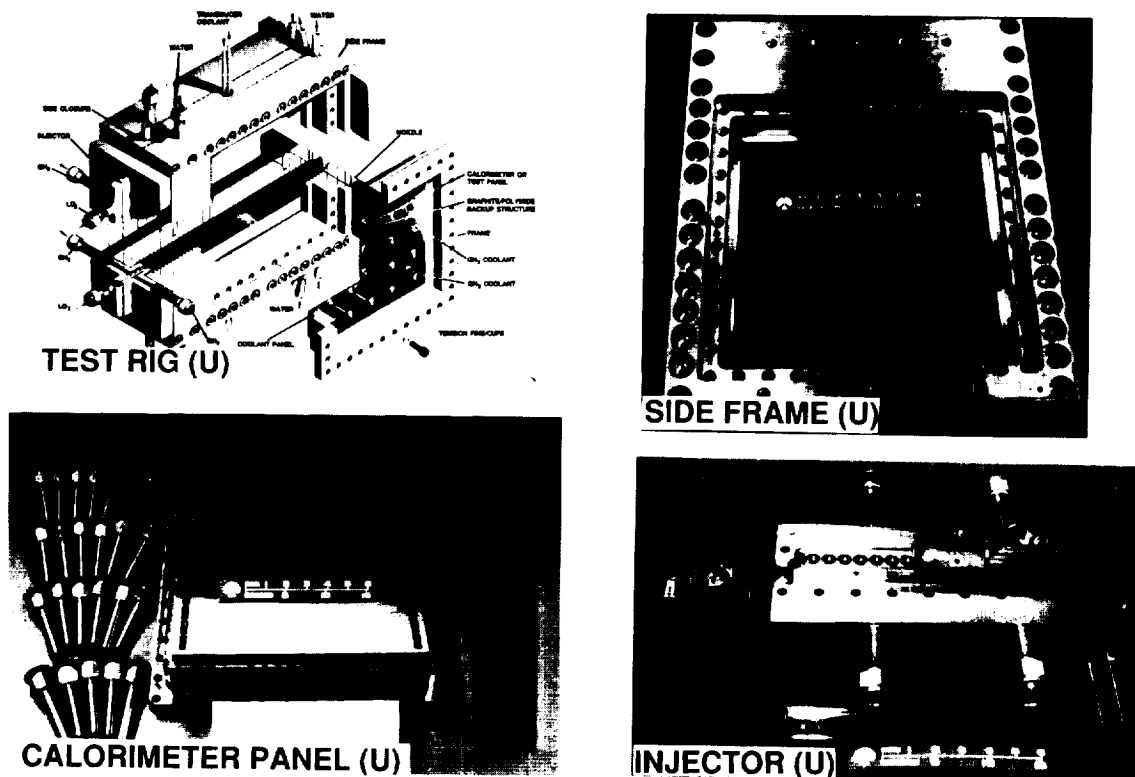


Figure 43

ORIGINAL PAGE
BLACK AND WHITE PHOTOGRAPH

MICROCHANNEL FABRICATION STUDIES

Very small grooves (microchannels) have been proposed as a means of reducing the weight of actively cooled panels and fabrication studies are underway. Microchannel grooves have been cut into Haynes 188, NARloy Z, and Incoloy 903 material using three fabrication processes; electric discharge machining (EDM), Electro-Chemical (ECM) etching and photoetching. Photographs of the channels are shown in figure 44. The microchannels are nominally .020-in.-wide by .010-in.-deep rectangles with a .003-in. radius on .038-in. centers for the EDM process, .023-in.-wide by .010-in.-deep ellipses on .034-in. centers for the ECM process and .020-in.-wide by .010-in.-deep semi-circles on .030-in. centers for the photoetching process.

EDM channels were cut into Haynes 188 by a subcontractor with a proprietary electrode and ECM channels were cut into Haynes 188 by a subcontractor using a proprietary etchant. Photoetching of Haynes 188 was unsuccessful. NARloy Z material could not be practically removed using the EDM process due to excessive tool wear, while ECM and photoetching processes exhibited varying degrees of success. A nitric acid solution was used as the etchant solution for the ECM process and a proprietary solution of ferric chloride and HCL was used as the etchant for the photoetching process. Using the photoetching process for NARloy Z resulted in the most repeatable channels and lands.

Channels were machined into Incoloy 903 using the EDM and the photoetching process. On the initial trial of the photoetch process a sludge formed in the Incoloy 903 channel prohibiting any further etching of the material. During the mechanical cleaning to remove the sludge, the photoresistant masking was inadvertently removed. The solution to keeping the masking attached to the surface of the Incoloy 903 was to slightly roughen the surface with a grit blast to provide adequate adhesion for the masking. Channels were then successfully cut into Incoloy 903 using a proprietary solution of ferric chloride and HCl. ECM of the Incoloy 903 panels is in progress. Details of the microchannel development are presented in reference 54.

(Figure 44 is shown on the next page.)

MICROCHANNEL FABRICATION DEVELOPMENT




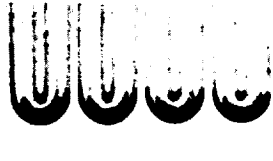


FAB METHOD MATERIAL	EDM	ELECTROCHEM ETCH	PHOTOETCH
HAYNES 188			• UNABLE TO ETCH
NARLOY Z	• TOOL WEAR UNACCEPTABLE		
INCOLOY 903		• IN PROGRESS	

Figure 44

ORIGINAL PAGE
BLACK AND WHITE PHOTOGRAPH

INCOLOY 909 DEMONSTRATOR PANEL

Early in the NASP Program an integral Incoloy 909 titanium actively cooled panel design was developed by Pratt and Whitney and Rohr Industries and the 20-inch-square demonstrator panel, shown in figure 45, was fabricated by Rohr Industries. The panel was designed to accommodate a heat flux of 320 Btu/ft²-sec, a hot gas surface pressure of 195 psi, a hydrogen coolant pressure of 1300 psi, and an acoustic load of 185 db with a maximum surface temperature of 1050° F. The panel features an Incoloy 909 heat exchanger and manifolds, sandwich panels on both the hot and cold sides of the assembly consisting of titanium 6-2-4-2 face sheets with 3-25 honeycomb core, and a titanium 6-2-4-2 egg crate type center structure.

There have been extensive correlations between results of dynamic structural analysis of the panel by Rohr Industries and tests of the panel by Pratt and Whitney. These correlations have included comparisons between results of finite element normal modes analysis and holographically measured mode shapes, and comparisons of predicted acoustic response with results of progressive wave tube tests at room temperature. The analysis considered sound sources and response mode shapes to 2500 hz, and accounted for partial structure exposure to the acoustic field, discrete frequency damping effects, and cross-modal coupled response. Despite the lack of rigorous structural damping data, there was good agreement between predicted and measured results.

An 8.9- by 9.0-inch, Incoloy 909 heat exchanger subcomponent panel was subjected to 15 thermal cycles at heating rate of 200 Btu/ft²-sec or greater (with a maximum flux of 260 Btu/ft²-sec) in the Wyle test facility with no evidence of panel damage.

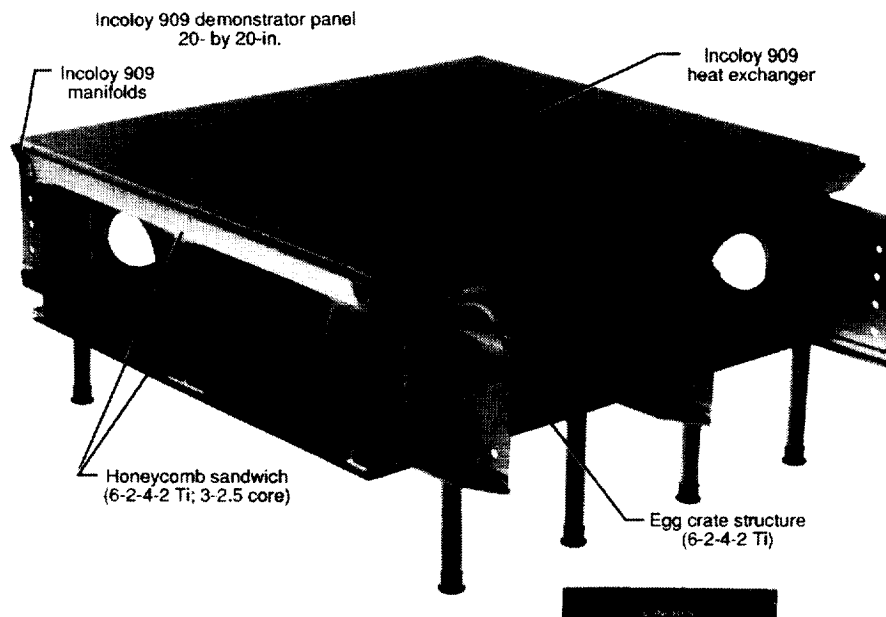


Figure 45

DEVELOPMENT OF C-SiC/REFRACTORY-METAL-TUBE HEAT EXCHANGERS

Considerable effort has gone into the development of a refractory-composite, skin-tube heat exchanger for a very high temperature, non-integral actively cooled structure. The primary incentive for this effort is to develop a cooled structure which can accommodate the very high heat fluxes encountered during ascent but does not require cooling during the more moderate (but still severe) heating during descent when the fuel/coolant is not available.

Based on initial material screening, design and optimization studies, and fabrication development efforts, carbon-silicon carbide was selected for the skin and Mo-50Re was selected for the tubes. The superior oxidation resistance of the silicon carbide matrix and compatibility of the coefficients of thermal expansion (CTE) of the tube and skin materials (relative to the other materials considered) were the primary factors leading to the material selections.

As indicated in figure 46 the continuing development of C-SiC/refractory-metal-tube heat exchangers has been a series of systematic studies involving both analytical and experimental efforts. The results, to date, have provided a detailed characterization of two-dimensional and three-dimensional C-SiC and refractory tubing materials, and have shown that through highly orthotropic tailoring, the mismatch of thermal expansion characteristic between the composite material and tubes can be minimized. The studies have established a data base for the materials, developed and demonstrated suitable fabrication techniques, and identified test techniques for validating the performance of the heat exchanger. Future plans include the fabrication and testing of a larger (8 in. by 12 in.) heat exchanger subcomponent. For additional details see references 54 and 55.

(Figure 46 is shown on the next page.)

DEVELOPMENT of C-SiC/REFRACTORY METAL-TUBE HEAT EXCHANGERS

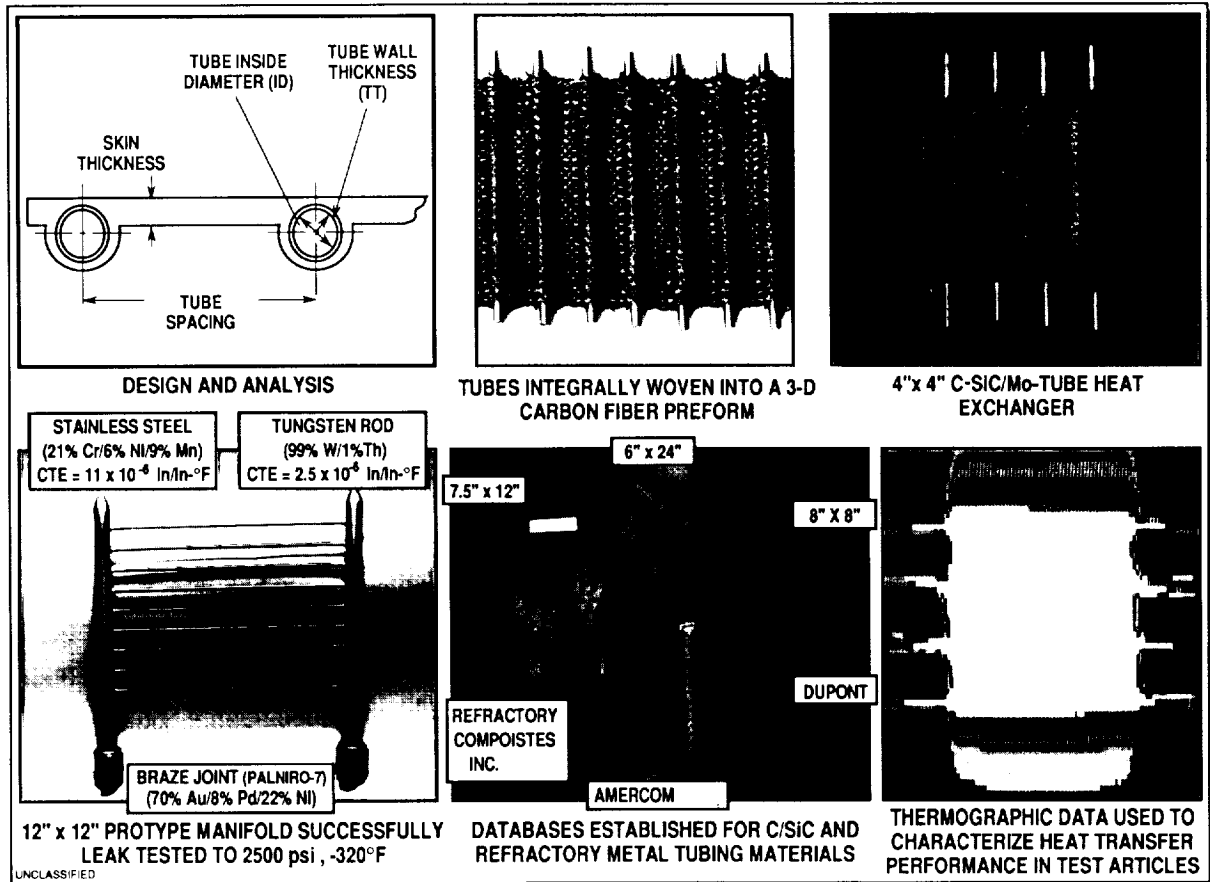


Figure 46

LESSONS LEARNED

A variety of important lessons (summarized in figure 47) have been learned from the actively cooled panels studies. In general, it can be said that the wide range of operational temperatures and the extremely hostile environment in which the panels are expected to operate tend to amplify the criticality of each element and add new dimensions to the design and development process. Seemingly minor details are important. For example, the use of non-perforated instead of perforated honeycomb core is believed to have been a factor in the catastrophic failure of the SiC/Ti panel. Similarly, a mismatch in thermal expansion characteristics was responsible for the Be skin/tube panel failure. Some of these critical details can be identified and resolved early by using small preliminary test specimens such as the joint fatigue specimens for the airframe structure panels. Material properties, which are sometimes considered secondary, (such as conductivity, thermal expansion, ductility, fracture toughness, etc.) assume primary importance because of the impact of heat transfer and the wide range of temperatures encountered. While not emphasized in the body of the paper, fabrication difficulties were encountered in the manufacture of each of the panels described in the paper. In contrast to uncooled structures which may function satisfactorily with less than perfect joints, the need for leak tight, unblocked coolant passages for cooled structures demands perfection in the fabrication process. Cleanliness is critical both in the fabrication process where foreign material or oxidation may produced substandard joints, and in operation where foreign material may block small coolant passages with potentially disastrous results. Current instrumentation techniques are inadequate for the hostile environment to which the hot surfaces of actively cooled panels are exposed. These hot surfaces often absorb large heat fluxes which may induce significant temperature gradients through-the-thickness of any instrumentation on that surface. Special techniques, perhaps optical, must be devised for hot surface strain and temperature measurements. Taken collectively the studies emphasize the need for testing through the entire anticipated operating range to uncover the "hidden flaws" which may occur in design or manufacturing.

Many critical concerns remain unresolved. Although the NASP studies did not progress to the point where fatigue life could be adequately investigated, it is known that thermal fatigue is a critical concern for actively cooled structures because of the large thermal stresses induced by the thermal gradients between the hot surface and the backside of the heat exchanger at the heat fluxes of concern. The present investigations also dramatically illustrate the importance of fracture toughness and thermal stress at low temperatures. Again, although not specifically addressed in the present paper but covered elsewhere during the tenth NASP Symposium, hydrogen and oxygen compatibility is a continuing concern. Finally, despite the advances in test facilities for actively cooled structures that have occurred under the auspices of the NASP Technology Maturation Program and the ongoing facility design and development activity, there is a pressing need to get higher heat flux facilities representative of engine environment checked-out and operational.

(Figure 47 is shown on the next page.)

LESSONS LEARNED

- DETAILS ARE IMPORTANT
- SECONDARY MATERIAL PROPERTIES ARE SIGNIFICANT
(CONDUCTIVITY, THERMAL EXPANSION, DUCTILITY,
FRACTURE TOUGHNESS)
- FABRICATION IS DIFFICULT
- CLEANLINESS IS CRITICAL
- INSTRUMENTATION IS INADEQUATE
- TESTING IS ESSENTIAL
- CRITICAL CONCERNS ARE
FATIGUE LIFE
FRACTURE TOUGHNESS
HYDROGEN AND OXYGEN COMPATIBILITY
FACILITIES

Figure 47

REFERENCES

1. Anon.: Conference on Hypersonic Aircraft Technology. NASA SP-148, Proceedings of a Conference held at Ames Research Center, Moffett Field, CA May 16-18, 1967.
2. Anon.: Recent Advances in Structures for Hypersonic Flight. NASA CP 2065, Proceedings of a Symposium held at Langley Research Center, Hampton, VA, September 6-8, 1978.
3. Staff of Langley Research Center and AiResearch Manufacturing Co., The Garret Corp.: Hypersonic Research Engine Project Technology Status 1971. NASA TMX-2572, September 1972.
4. Wieting, Allan R.: Aerodynamic and Thermal Analysis of Results of Tests of a Hydrogen-Cooled Scramjet Engine, (HRE-SAM) at Mach 6.3. NASA TMX-2767, May 1973.
5. Anon.: First National Aero-Space Plane Technology Conference, NASP CP 1006, Vol. VI, May 1986.
6. Kelly, H. N.; Mezines, S. A.; Purmort, W. P.; Henson, M. C.; Warburton, R. E.; and Phelps, J. D.: Actively-Cooled Panels. Presented at the Tenth National Aero-Space Plane Technology Symposium, Paper Number 154, April 23-26, 1991.
7. Kelly, H. Neale; and Sikora, Timothy P.: Actively Cooled Panel Testing Perils, Problems, and Pitfalls. Presented at the SEM Structural Testing Technology at High Temperatures Conference, Dayton, OH, November 4-6, 1991.
8. Anthony, Frank M.; and Huff, Roland D.: Analytical Evaluation of Actively Cooled Modified Monocoque Structural Sandwich Concepts. Technical Report AFFDL-TR-65-124, July 1965.
9. Atkins, T. G.: Hypersonic Ramjet Heat Transfer and Cooling Program. Volume I: Results of Regenerative Cooling Experiments. Technical Report AFAPL-TR-66-84, Vol. I, August 1966.
10. Flieder, W. G.; Richard, C. E.; Buchmann, O. A.; and Walters, F. M.: An Analytical Study of Hydrogen Cooled Panels for Application to Hypersonic Aircraft. NASA CR-1650, April 1971.
11. Walters, F. M. and Buchman, O. A.: Heat Transfer and Fluid Flow Analysis of Hydrogen-Cooled Panels and Manifold Systems. NASA CR-66925, July 1970.
12. Demogenes, C.; Jones, O.; Richard, C. E.; Duncan, J. D.; and Flieder, W. G.: Fabrication and Structural Evaluation for Regeneratively Cooled Panels. NASA CR-1651, March 1971.

13. Richard, C. E.; Duncan, J. D.; Demogenes, C.; and Flieder, W. G.: Low-Cycle Fatigue Evaluation for Regeneratively Cooled Panels. NASA CR-1884, October 1971.
14. Richard, C. E.; and Walters, E. M.: Comparison of Hydrogen and Methane as Coolants in Regeneratively Cooled Panels. NASA CR 1652, March 1971.
15. Richard, C. E.; Duncan, J. D.; Gellersen, E. W.; and Demogenes, C.: Thermal and Structural Tests of a Hydrogen Cooled Panel. NASA CR 2105, August 1972.
16. Jilly, L. F., Editor: Hypersonic Research Engine Project - Phase II Aerothermodynamic Integration Model Development. NASA CR-132654, May 1975.
17. Jilly, L. F., Editor: Hypersonic Research Engine Project - Phase II Structures Assembly Model (SAM) Test Report. NASA CR-111993, September 1971.
18. Henry, John R. and Anderson, Griffin Y.: Design Considerations for the Airframe - Integrated Scramjet. Presented at the First International Symposium on Air Breathing Engines, Marseille, France, June 19-23, 1972. (Also published as NASA TMX-2895, December 1973.)
19. Wieting, Allan R. and Guy, Robert W.: Preliminary Thermal Structural Design and Analysis of an Airframe-Integrated Hydrogen-Cooled Scramjet. AIAA Paper 75-137, Pasadena, CA, 1975. (Also published as Journal of Aircraft, Vol. 13, March 1976, pp. 192-197.)
20. Kelly, H. Neale; Wieting, Allan R.; Shore, Charles P.; and Nowak, Robert J.: Recent Advances in Convectively Cooled Engine and Airframe Structures for Hypersonic Flight. Presented at the Eleventh Congress of the International Council of the Aeronautical Sciences (ICAS), Lisbon, Portugal, Sept. 1978. (Also published as NASA CP-2065, September 1978.)
21. Buchman, O. A.: Thermal-Structural Design Study of an Airframe-Integrated Scramjet - Summary Report. NASA CR-3141, October 1979.
22. Killackey, J. J.; Katinszky, E. A.; Tepper, S.; Vuigner, A. A.; Wright, C. C.; and Stockwell, G. G.: Thermal-Structural Design Study of an Airframe-Integrated Scramjet - Final Report. NASA CR-159039, May 1980.
23. Buchman, O. A.; Arefin, V. V.; Warren, H. A.; Vuigner, A. A.; and Pohlman, M. J.: Advanced Techniques for Hydrogen-Cooled Engine Structures. NASA CR-3949, September 1985.
24. Jilly, L. F., Editor: Hypersonic Research Engine Project - Phase II Structures and Cooling Development. Final Technical Data Report NASA CR-112087, May 1972.
25. McConarty, W. A. and Anthony, F. M.: Design and Evaluation of Active Cooling Systems for Mach 6 Cruise Vehicle Wings. NASA CR-1916, 1971.

26. Helenbrook, R. G.; McConarty, W. A.; and Anthony, F. M.: Evaluation of Active Cooling Systems for a Mach 6 Hypersonic Transport Airframe. NASA CR-1917, 1971.
27. Helenbrook, R. G.; and Anthony, F. M.: Design of a Convective Cooling System for a Mach 6 Hypersonic Transport Airframe. NASA CR-1918, 1971.
28. Anthony, F. M.; Dukes, W. H.; and Helenbrook, R. G.: Internal Convective Cooling Systems for Hypersonic Aircraft. NASA CR-2480, 1974.
29. Brewer, G. D.; and Morris, R. E.: Study of Active Cooling for Supersonic Transports. NASA CR-132573, 1975.
30. Pirrello, C. J.; Baker, A. H.; and Stone, J. E.: A Fuselage/Tank Structure Study for Actively Cooled Hypersonic Cruise Vehicles - Summary. NASA CR-2551, 1976.
31. Nowak, Robert J.; and Kelly, H. Neale: Actively Cooled Airframe Structures for High-Speed Flight. Presented at the AIAA/ASME/SAE 17th Structures, Structural Dynamics and Materials Conference, King of Prussia, PA, May 5-7, 1975. (Also Journal of Aircraft, Vol. 14, No. 3, March 1977, pp. 244-250.)
32. Koch, L. C.; and Pagel, L. L. : High Heat Flux Actively Cooled Honeycomb Sandwich Structural Panel for a Hypersonic Aircraft. NASA CR-2959, 1978.
33. Pirrello, C. J.; and Herring, R. L.: Study of a Fail-Safe Abort System for an Actively Cooled Hypersonic Aircraft - Volume I, Technical Summary. NASA CR-2562, January 1976.
34. Herring, R. L.; and Stone, J. E.: Thermal Design for Areas of Interference Heating on Actively Cooled Hypersonic Aircraft. NASA CR-2828, December 1976.
35. Ellis, D. A.; Pagel, L. L.; and Schaeffer, D. M.: Design and Fabrication of a Radiative Actively Cooled Honeycomb Sandwich Structural Panel for a Hypersonic Aircraft. NASA CR-2957, March 1978.
36. Jones, R. A.; Braswell, D. O.; and Richie, C. B.: Fail-Safe System for Actively Cooled Supersonic and Hypersonic Aircraft. NASA TMX-3125, 1975.
37. Anthony, F. M.: Design and Fabrication of a Skin Stringer Discrete Tube Actively Cooled Structural Panel. NASA CP-2065, September 1978.
38. Smith, L. M.; and Beuyukian, C. S.: Actively Cooled Plate Fin Sandwich Structural Panels for Hypersonic Aircraft. NASA CR-3159, August 1979.
39. Shore, Charles P. and Weinstein, Irving: Aerothermal Performance of a Radiatively and Actively Cooled Panel at Mach 6.6. NASA TP-1595, December 1979.
40. Shore, Charles P.; Nowak, Robert J.; and Kelly, H. Neale: Flightweight Radiantly and Actively Cooled Panel - Thermal and Structural Performance. NASA TP-2074, October 1982.

41. Webb, Granville; Clark, Ronald K.; and Sharpe, Ellsworth L.: Thermal Fatigue Tests of a Radiative Heat Shield Panel for a Hypersonic Transport. NASA TM-87583, September 1985.
42. Blosser, Max L.; Nowak, Robert J.; and Rothgeb, Timothy M.: Thermal-Structural Tests of a Water/Glycol Cooled Aluminum Panel. Workshop on Correlation of Hot Structures Test Data with Analysis, November 1988, NASA CP 3065, Vol. I, pp. 158-178.
43. Purmort, Paul: NASP Technical Option 3 - Actively Cooled Primary Structures - Final Report. Rockwell International report NA-90-101 prepared under contract F33657-86-C-2127, May 1991.
44. Mezines, Sam: Generic Option No. 3 - Actively Cooled Metallic Primary Structure. NASP CR-1123, October 1991. Final Report Addendum. MDC Q0962, October, 1991.
45. Clay, Chris: Nose Cap Technology Developments. Paper No. 159, Tenth National Aero-Space Plane Technology Symposium, Monterey, CA, April 23-26, 1991.
46. Camarda, Charles J.: Results of Generic Studies of Leading Edges. Paper No. 155, Tenth National Aero-Space Plane Technology Symposium, Monterey, CA, April 23-26, 1991.
47. Bolser, David; Sullivan, Steve: Experiences in Fabricating Actively Cooled Structures. Fifth National Aero-Space Plane Technology Symposium, October 1988, NASP CP-5033, Vol. VI, pp. 267-296.
48. Popp, Robert; and Mezines, Sam: Recent Developments in Testing Actively Cooled Structures: Part 2 - Test Results. Fifth National Aero-Space Plane Technology Symposium, October 1988, NASP CP-5033, Vol. VI, pp. 321-350.
49. Mezines, S. A.: Actively Cooled Panel Test Results. Seventh National Aero-Space Plane Technology Symposium, October 1989, NASP CP 7045, Vol. VI, pp. 209-240.
50. Brammer, Donald; Capshaw, Norman; and Sikora, Timothy: Recent Developments in Testing Actively Cooled Structures: Part I -Testing. Fifth National Aero-Space Plane Technology Symposium, October 1988, NASP CP-5033, Vol. VI, pp. 297-320.
51. Smith, Drexel L.: Actively Cooled Hydrogen Test Facility, Paper No. 134, Tenth National Aero-Space Plane Technology Symposium, Monterey, CA, April 23-26, 1991.
52. Haller, Gerald R.; and Mezines, S. A.: Failure Analysis of Beryllium Skin/Tube Actively-Cooled Panel. Eighth National Aero-Space Plane Technology Symposium, March 1990, NASP CP 8051, pp. 149-170.

53. Vrable, Daniel L.; and Beavers, Fred L.: Design and Fabrication of Actively Cooled Gr/Cu Structures. Seventh National Aero-Space Plane Technology Symposium, October 1989, NASP CP-7045, Vol. VI, pp. 183-208.
54. Phelps, John D.; Kelly George J.; and Gersley, Jim G.: Microchannel Heat Exchanger Design for Hypersonic Engine Actively Cooled Flowpath Structure. Ninth National Aero-Space Plane Technology Symposium, November 1990, NASP CP-9057, Vol. VI, pp. 123-147.
55. Henson, M. C.; Adams, R. D.; Ahmad, A.; Fetter, S. D.; Kennedy, S. E.; Saathoff, W. M.; and Serinken, D. H.: Development of Refractory Composite Actively Cooled Panels for the NASP Airframe. Ninth National Aero-Space Plane Technology Symposium, November 1990, NASP CP 9057, Vol. VI, pp. 149-174.

